



Published in final edited form as:

Chem Res Toxicol. 2012 September 17; 25(9): 1842–1861. doi:10.1021/tx3000494.

Intramolecular hydrogen transfer reactions of thiyl radicals from glutathione: formation of carbon-centered radical at Glu, Cys and Gly

Olivier Mozziconacci[†], Todd D. Williams[‡], and Christian Schöneich^{†,*}

[†]Department of Pharmaceutical Chemistry, 2095 Constant Avenue, University of Kansas, Lawrence, KS 66047

[‡]Laboratory of Mass Spectrometry, University of Kansas, Lawrence, KS 66045

Abstract

Glutathione thiyl radicals (GS^{*}) were generated in H₂O and D₂O by either exposure of GSH to AAPH[#], photoirradiation of GSH in the presence of acetone, or photoirradiation of GSSG. Detailed interpretation of the fragmentation pathways of deuterated GSH and GSH-derivatives during mass spectrometry analysis allowed us to demonstrate that reversible intramolecular H-atom transfer reactions between GS^{*} and C-H bonds at Cys[^αC], Cys[^βC], and Gly[^αC] are possible.

Keywords

glutathione; thiyl radical; C-centered radical; hydrogen transfer; mass spectrometry

1. Introduction

The tripeptide glutathione (GSH) plays a critical role in cellular homeostasis.¹ GSH is an essential component of (i) the glutathione-S-transferase-catalyzed conjugation affording signalling and regulation of biological pathways,² xenobiotic detoxification³ and (ii) cellular redox homeostasis through reversible oxidation to glutathione disulfide (GSSG; reaction 1).⁴



[#]Abbreviations: NEM: N-ethylmaleimide; IOA: Iodoacetamide; AAPH: 2,2'-azobis(2-methylpropionamide) dihydrochloride; GSH^{*}: Reduced-glutathione, where Gly residue is labeled with ¹⁵N and ¹³C at carbons C₁ and C₂.

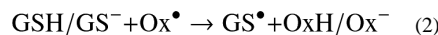
MSⁿ fragmentation (n=1,2,3,4): An ion trap mass spectrometer equipped with multiple quadrupoles can perform multiple stage mass spectrometry (MSⁿ). Therefore, this symbol refers to multi-stage MS/MS experiments designed to record product ion spectra where n is the number of product ion stages. The latter is so-called, progeny ion, and corresponds to a charged product of a series of consecutive reactions that includes product ions, at the 1st generation, 2nd generation and etc... According to the sequential fragmentation: M₁⁺ → M₂⁺ → M₃⁺ → M₄⁺ → M₅⁺, M₄⁺ is the precursor ion of M₅⁺, a 1st generation product ion of M₃⁺, but also a 2nd generation product ion of M₂⁺ and a 3rd generation product ion of M₁⁺. Thus, the fragmentation of the M₄⁺ ion is obtained at the MS⁴ stage.

*Corresponding Author: Schöneich, C.: Department of Pharmaceutical Chemistry, 2095 Constant Avenue, University of Kansas, Lawrence, KS 66047; fax, (785) 864-5736; schoneic@ku.edu.

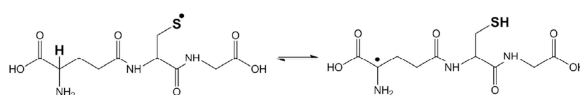
Associated content

Supporting Information. Sections S1-S6, describing MS³ and MS⁴ fragmentation pathways, DFT calculations of the fragmentation pathway of intermediate I₁, Schemes S1-S4, and Figure S1. This material is available free of charge via the Internet at <http://pubs.acs.org>.

GSH is also a suitable hydrogen/electron donor for one-electron reduction reactions, which lead to glutathione thiyl radicals, GS^\bullet (reaction 2).



Such one-electron reduction reactions of thiols are relevant for the protection of organisms against free radicals, generated, for example, through metabolic processes⁵ or the exposure to ionizing radiation.⁶ However, it was recognized that thiyl radicals may also involve in the reverse reaction, i.e. hydrogen abstraction from C-H bonds present in alcohols and ethers,⁷⁻¹⁰ carbohydrates,¹¹ polyunsaturated fatty acids,¹² and amino acids,¹³⁻¹⁵ and rate constants for such reactions have been provided by means of radiation chemical techniques. In peptides the resulting carbon-centered radicals can involve in hydrogen transfer reactions between amino acid side chains.¹⁶



(3)

Specifically GS^\bullet radicals feature a pH-dependent *intramolecular* hydrogen transfer between the thiyl radical moiety and the $^\alpha$ C-H bond of the N-terminal γ -Glu residue (reaction 3).^{13,17,18} However, electron spin resonance (ESR)^{19,20} and pulse radiolysis studies²¹ have also demonstrated evidence for hydrogen transfer between the thiyl radical and additional C-H bonds. For example, Karoui et al.²⁰ demonstrated that the oxidation of GSH resulted in the appearance of two types of carbon-centered radicals, monitored by ESR, and Neta and Fessenden¹⁹ interpreted their ESR data with the formation of a carbon-centered radical at the $^\alpha$ C position of the Cys residue. The latter observation would suggest the possibility for a 1,3-hydrogen transfer in GS^\bullet , supported also by experimental observations on the oxidation of penicillamine.²⁰ Additional ESR experiments obtained with small model thiols also suggest the possibility for a formal 1,2-hydrogen transfer in thiyl radicals, i.e. the observation of $^\bullet$ CH₂SH radicals after the photolysis of CH₃SH,²² and the detection of CH₃C $^\bullet$ H-SH radicals after photolysis of CH₃CH₂SH.²³

Theoretical calculations have examined activation energies for *intramolecular* hydrogen transfer reactions in GS^\bullet .²⁴ Here, the hydrogen transfer between the thiyl radical and the $^\alpha$ C-H bond of γ -Glu displays a rather low activation energy of $\Delta G = 37-42 \text{ kJ mol}^{-1}$, whereas the 1,3-hydrogen shift within the Cys residue shows $\Delta G = 110 \text{ kJ mol}^{-1}$ and hydrogen transfer from the C-H bonds of the C-terminal Gly residue shows $\Delta G = 134 \text{ kJ mol}^{-1}$ (in the (Z)-conformation). Nevertheless, experimental evidence for a 1,3-hydrogen transfer within thiyl radicals from Cys (CysS $^\bullet$) exists, both in the gas phase²⁵ and in solution.^{13,26} In addition, covalent H/D exchange experiments have demonstrated the potential for CysS $^\bullet$ radicals to abstract hydrogen atoms from neighbouring Gly and Ala residues in several model peptides,²⁷⁻³¹ suggesting that such a hydrogen transfer reactions should, in principle, be experimentally possible also in GS^\bullet .

In this paper, we report experimental evidence that the thiyl radical in GS^\bullet enters reversible hydrogen transfer reactions not only with the γ -Glu residue, but to a significant extent with the C-H bonds of Cys (1,2- and 1,3-hydrogen transfer) as well as the C-terminal Gly residue. To demonstrate these hydrogen transfer reactions, we have generated GS^\bullet via three

independent chemical methods, (i) the reaction of GSH with carbon-centered radicals generated through the thermal decomposition of (AAPH), (ii) the photolysis of GSSG, and (iii) the reaction of GSH with carbon-centered radicals ($\cdot\text{CH}_3$, $\text{CH}_3\text{C}\cdot\text{O}$) generated through the photolysis of acetone. Reversible hydrogen transfer reactions were monitored through covalent H/D exchange reactions of original C-H bonds, analysed by mass spectrometry, including MS^2 , MS^3 , and MS^4 experiments[#]. An important experimental result is the ultimate conversion of the GSH Cys residue into dehydroalanine (Dha), likely via β -elimination following a 1,3-hydrogen transfer of the initial thiyl radical, a mechanism recently established for small Cys-containing model peptides.³² Dha represents an important electrophile with the potential to generate thioether cross-links with excess GSH or protein thiols.³³

2. Materials and Methods

2.1 Materials

Reduced glutathione (GSH), oxidized glutathione (GSSG), ammonium bicarbonate (NH_4HCO_3), 2,2'-azobis(2-methylpropanimidine) dihydrochloride (AAPH), N-ethylmaleimide (NEM), iodoacetamide (IOA) and acetone were supplied by Sigma-Aldrich (St Louis, MO) at the highest purity grade. Stable isotope-labeled glutathione (GSH*, here the Gly residue is labeled with ^{15}N , and ^{13}C at carbons C_1 and C_2), deuterated acetone (acetone- d_6 , 99.9%) and deuterium oxide (D_2O , 99.9%) were purchased at Cambridge Isotope Laboratories (Andover, MA). The structures of GSH, GSH*, and GSSG are presented in Chart 1.

2.2 Preparation of the deuterated buffer solutions

Ammonium bicarbonate buffers were prepared at a concentration of 50 mM at three different pH/pD, 7.1, 8.1, and 9.1. The deuterated buffers were obtained by dilution of NH_4HCO_3 salt (19.2 mg) in pure D_2O (1 mL) and repetition (3 times) of the following procedure: i) vacuum drying of D_2O , ii) reconstitution into 1 mL D_2O . After the final vacuum drying step, ND_4DCO_3 was resolubilized into 5 mL D_2O . In parallel, a stock solution of KOD (0.1 M) was prepared in D_2O according to the same protocol. KOD stock solution was used to adjust the pD of ND_4DCO_3 buffer solutions.

2.3 Reaction between GSH and AAPH

GSH (750 μM) and AAPH (2 mM) were incubated for 1 hour at 37 °C under Ar in ammonium bicarbonate buffers (50 mM, pH/pD 7.1, 8.1 or 9.1). The stock solutions of GSH and AAPH were pre-saturated under Ar and placed on ice prior to be mixed. The reaction was stopped by alkylation of Cys with NEM. The latter was performed as follows: the samples were diluted in 50 mM ammonium bicarbonate, pH 8, in 50:50 (v/v) $\text{H}_2\text{O}/\text{D}_2\text{O}$ (referred to as balanced ammonium bicarbonate; for a rationale to use balanced buffer, see section 2.9) containing 1 mM NEM. The reaction products were analyzed by capillary LC-MS/MS connected to a SYNAPT-G2 (Waters Corporation, Milford, MA, USA) mass spectrometer (for more details on LC-MS analysis, see section 2.7).

2.4 Reaction between GSH* and AAPH

GSH* (750 μM) and AAPH (2 mM) were incubated for 1 hour at 37 °C under Ar in a non-buffered solution. The amount of GSH* was limited. To run MS^n experiments on the GSH*-derived products, we had to maintain a concentration of GSH* similar to that used with GSH. Experimentally, the latter led us to avoid dilution of the GSH* stock solution. The pH of the solution was therefore different from the pH of the other solution (GSH). Because in this pH range the decomposition rate of AAPH may vary, our experiments will not allow us

to compare quantitatively the amount of covalent deuterium incorporation into GSH* (vs GSH). GSH* was only used, in parallel to GSH, to discriminate between the different fragment ions during the MSⁿ experiments. By no means the GSH* solution could be used for quantitative measurements. The pH/pD of the final solutions was 3.5 (after addition of AAPH). The stock solutions of GSH* and AAPH were pre-saturated with Ar, and placed on ice prior to be mixed. The reaction was stopped by alkylation of Cys with either NEM or IOA. The chemical derivatizations were performed as follows: 100 μL of each sample were diluted either with 900 μL of milliQ H₂O (if the sample was incubated in H₂O) or with 900 μL D₂O (if the sample was incubated in D₂O) which both contained 1 mM of either NEM or IOA. The pH/pD of each solution was adjusted to 8.0 by addition of KOH (or KOD). The derivatized products GSH*-NEM and GSH*-IOA were analyzed by mass spectrometry using a Fourier Transform Ion Cyclotron Resonance (FT-ICR) instrument (for more details, see section 2.8).

2.5 UV-irradiation of GSSG

GSSG (500 μM) was photo-irradiated in H₂O and D₂O for 10 min at $\lambda = 253.7$ by means of a photo-irradiator (RayonetTM, Southern New England, Branford, CT, RMA-500) equipped with four UV lamps (RMR-2537Å) with a flux of 3.2×10^{-7} einstein/sec. Prior to UV-irradiation, a 300 μL aliquot of each H₂O and D₂O solution containing GSSG (500 μM) in ammonium bicarbonate buffer (50 mM, pH/pD 7.1, 8.1 or 9.1) was placed in a quartz tube and saturated with Ar. After photo-irradiation the samples were diluted into a balanced ammonium bicarbonate buffer containing 1 mM NEM (the balanced buffer is described in section 2.9). The products of UV-irradiation were analyzed by capillary LC-MS connected to a SYNAPT-G2 mass spectrometer (Waters Corporation, Milford, MA, USA).

2.6 Acetone-h₆ and acetone-d₆ photochemistry in the presence of GSH and GSH*

GSH and GSH* (500 μM) were prepared in 1 mL solutions consisting of acetone-h₆:H₂O (20%:80% v:v) or acetone-d₆:H₂O (20%:80% v:v), respectively. The solutions were pre-saturated with Ar prior to photo-irradiation for 10 min at $\lambda = 253.7$ by means of a photo-irradiator (RayonetTM, Southern New England, Branford, CT, RMA-500) equipped with four UV lamps with a flux of 3.2×10^{-7} einstein/sec. The photo-irradiated samples were diluted by adding 100 μL of each to 900 μL of milliQ H₂O prior to FT-ICR mass spectrometry analysis.

2.7 Sample preparation for capillary LC-MS analysis connected to a SYNAPT-G2 mass spectrometer

10 μL of the sample were injected onto a Vydac column (25 cm \times 0.5 mm C18, 3.5 μm), and eluted with a linear gradient delivered at a rate of 20 $\mu\text{L min}^{-1}$ by a Capillary Liquid Chromatography System (Waters Corporation, Milford, MA, USA). Mobile phases consisted of water/acetonitrile/formic acid at a ratio of 99%, 1%, 0.08% (v:v:v) for solvent A and a ratio of 1%, 99%, 0.06% (v:v:v) for solvent B. The following linear gradient was set: 1–50% of solvent B within 15 min. Electrospray ionization (ESI) MS spectra of the photoproducts were acquired on a SYNAPT-G2 (Waters Corporation, Milford, MA), operated for maximum resolution with all lenses optimized on the $[\text{M} + 2\text{H}]^{2+}$ ion from the $[\text{Glu}]^1$ -fibrinopeptide B. The cone voltage was 30 V and Ar was admitted to the collision cell. The spectra were acquired using a mass range of 50–2000 amu. The data were accumulated for 0.7 sec per cycle.

2.8 Sample preparation for FT-ICR analysis

The following procedure was applied to analyze products obtained from i) the acetylation and deuterium-acetylation of GSH and GSH* during photo-irradiation in the presence of

acetone- h_6 and acetone- d_6 , and ii) the covalent deuterium incorporation into GSH* during exposure to AAPH in D_2O . Here the derivatization of GSH/GSH* with NEM or IOA was performed in 100% of D_2O before dilution (1/100) into H_2O :formic acid (99.9%:0.1%, v:v) to allow H/D-exchange of mobile protons/deuterons. Collision induced dissociation (CID) of fragment ions, referred to as MS^3 and MS^4 , was performed by means of an LTQ-FT hybrid linear quadrupole ion trap Fourier transform ion cyclotron resonance (FT-ICR) mass spectrometer (ThermoFinnigan, Bremen, Germany)³⁴. MS^3 and MS^4 were acquired with an attenuation of the parent ion in the range of 25%-35%. The mass window to collect the parent ion was fixed to 0.2 Da. The samples were directly infused.

2.9 Covalent H/D exchange into GSH/GSH* and isotopic correction

After exposure of GSH to AAPH or formation of GSH during photoirradiation of GSSG, covalent deuterium incorporation into GSH (and GSH*) was determined as described below.

The formation of GSH during the photo-irradiation of GSSG and the mechanisms leading to covalent deuterium incorporation into GSH are described in Scheme 1. Briefly, UV-irradiation at $\lambda = 253.7$ nm of a disulfide bond (as in GSSG) leads to the formation of a pair of thiyl radicals (GS^\bullet). Ultimately, the disproportionation reaction of two GS^\bullet radicals leads to the formation of a thiol and a thioaldehyde. More details about the photochemistry of disulfide bonds are documented elsewhere.^{28,30,35} The reaction of GSH with AAPH (Scheme 1, reactions 4 and 5) leads to the formation of GS^\bullet .¹¹ Intramolecular H-atom transfer between GS^\bullet and one of the several C-H bonds present in GS^\bullet (Scheme 1, reaction 7) generates C-centered radicals and a thiol, which converts into deuteriothiol in D_2O , and donates a deuterium back to the carbon-centered radical (Scheme 1, reactions 8 and 9).

After derivatization with NEM, the deuterium composition of GS-NEM and its fragment ions was determined from the differences between the average mass of a covalently deuterated peptide and the average mass of the corresponding fully protonated peptide. The average masses were calculated from centroided isotopic distributions. The distribution of deuterium incorporation is obtained after isotopic correction by subtracting the isotope abundance distribution in the product formed during either exposure to AAPH or UV-irradiation in H_2O from the isotope abundance distribution of the same product generated in D_2O . This variation of the isotopic distribution between the experiments performed in D_2O and H_2O will be given throughout this paper by the variation of the percent base peak intensity (% Δ BPI).

Importantly, the derivatization of GSH with NEM in D_2O leads to the incorporation of one deuterium into the derivatized photoproduct (GS-NEM). In order to minimize quantitative errors, and in order to compare GSH/GSH* isolated from reactions in H_2O and D_2O , all NEM derivatizations were performed in balanced ammonium bicarbonate buffer (i.e., 50/50 H_2O/D_2O , v/v), where either H_2O samples were supplemented with D_2O , or D_2O samples were supplemented with H_2O (see section 2.3). This method of balanced buffer was successfully applied previously to monitor covalent H/D exchange of several peptides and proteins.²⁷⁻³⁰ Consequently, any differences in covalent deuterium content in GSH/GSH* are the result of the free radical reactions (and not the derivatization with NEM).

2.10 Computational details

Density Functional Theory (DFT) calculations presented were performed with the Gaussian-03 (G03) molecular orbital packages. The geometry optimization and frequency calculations were carried out at the B3LYP/6-311+G(d,p) level by the hybrid HF-DFT procedure implemented in the Gaussian software package.³⁶ The geometries of the

molecules were optimized in vacuum. The Gibbs free energies were calculated at 298°K (G_{298}^0) and are given in kcal/mol.

3. Results

Three chemical routes for the formation of glutathione thiyl radicals (GS^\bullet) were used (Scheme 1). The first route consisted of exposing GSH (or GSH^*) to the C-centered radical resulting from the thermal decomposition of AAPH. Such reaction allows H-atom abstraction from the thiol to generate GS^\bullet (Scheme 1, reactions 4 and 5). The second and third routes are based on photochemical techniques. The photoirradiation of GSSG at $\lambda=253.7$ nm yields a pair of thiyl radicals (Scheme 1, reaction 6), analogous to processes characterized for various peptide disulfides.^{28,30,35} The photochemistry of acetone yields methyl and acetyl radicals (Scheme 1, reaction 10). GSH (and GSH^*) reacts with $^\bullet CH_3/^\bullet CD_3$, and $^\bullet COCH_3/^\bullet COCD_3$ generated during the photochemistry of acetone- h_6 or acetone- d_6 , respectively, which initially abstract the H-atom from the thiol function of GSH (or GSH^*). Subsequently, covalent H/D exchange reactions (Scheme 1, reactions 7–9) were monitored, and, in addition, the final recombination products of glutathione-derived radicals (either C- or S-centered radicals) with the acetyl radical (Scheme 1, reactions 11–13). Using a combination of GSH/ GSH^* and CX_3CO ($X=H,D$) in H_2O provided a number of variables to identify specific products characteristic for radical formation on glutathione after initial formation of GS^\bullet .

3.1 GSH and the thermal decomposition of AAPH

GSH (m/z 308.1) was incubated under Ar for 1 hour in the presence of AAPH in H_2O and D_2O . Subsequently, GSH was derivatized with NEM in a balanced mixture of H_2O/D_2O at pH/pD 8.0 (See sections 2.3 and 2.9). The GS-NEM derivatives obtained after reaction of GSH with AAPH in H_2O and with AAPH in D_2O will be referred to as products **1-h** and **1-d-X**, respectively (summarized in Table 1). The label **X** in the series of products **1-d** (**X** = Cys[^{13}C], Cys[^{34}S], or Gly[^{13}C]) represents deuterium incorporation at Cys[^{13}C], Cys[^{34}S], or Gly[^{13}C], respectively.

Analysis by MS¹ and MS²—The comparison of the isotopic distributions of the parent ions of **1-h** and **1-d-X** (m/z 433.14) obtained after exposure of GSH to AAPH in H_2O (Fig. 1, A) and in D_2O (Fig. 1, B), respectively, shows a shift toward higher masses. This observation indicates that deuterium atoms are covalently incorporated into GSH during the exposure to AAPH in D_2O . The deconvolution of the isotopic distributions of **1-h** and **1-d-X** obtained after reactions with AAPH in the range of pH/pD 7.1 – 9.1, shows that 37% – 41% of the molecules have incorporated one deuterium (Fig. 1, inserted table). The MS/MS analysis of **1-h** and **1-d-X**, and the comparison of the isotopic distributions of their b2 (m/z 358.1) and y2 (m/z 304.1) fragment ions, show that deuterium incorporation occurs to an equal extent in the subsequences $^{\gamma}Glu$ -Cys and Cys-Gly, respectively (Fig. 2). The fragment ion with m/z 102.05, corresponding to the $^{\gamma}Glu$ residue, shows covalent deuterium incorporation.

3.2 GSH^* and the thermal decomposition of AAPH

GSH^* (m/z 311.1) was incubated under Ar for 1 hour in the presence of AAPH in H_2O and D_2O in non-buffered solutions. Subsequently, GSH^* was derivatized with either NEM or IOA in either H_2O or D_2O at pH/pD 8.0 (See sections 2.4 and 2.9). The GS-NEM derivative products obtained after reaction of GSH^* with AAPH in H_2O and D_2O , respectively will be referred to as products **2-h** and **2-d-X**, respectively (Table 2). The GS-IOA derivative products obtained after reaction of GSH^* with AAPH in H_2O and D_2O will be referred to as products **3-h** and **3-d-X**, respectively (Table 3). The label **X** (= Cys[^{13}C], Cys[^{34}S], or

Gly[^{13}C]) in the series of products **2-d** and **3-d** represents deuterium incorporation at Cys[^{13}C], Cys[^{13}C], or Gly[^{13}C], respectively.

First, ^{15}N and ^{13}C labeling of the Gly* residue in GSH* allows several fragments to be distinguished during MS/MS analysis, such as the immonium ion from Cys (m/z 76.05) and the y1 fragment (= Gly*, m/z 79.05). Second, the ^{13}C label in the carboxylic acid group of Gly* will allow us to detect the loss of ^{13}CO (MW = 29 Da) during MS³ fragmentation.

MS³ analysis of product 2-d-X—After the reaction of GSH* with AAPH in H₂O and D₂O, and derivatization of GSH* with NEM, a comparison of the MS¹ spectra of the products **2-h** (m/z 436.1) and **2-d-X** (m/z 438.1 and 439.1) indicate the incorporation of two (m/z 438.1) and three (m/z 439.1) deuterons into product **2-d-X**. To localize the deuterium atoms in **2-d-X**, an MS³ analysis of the y2 fragment ions was performed. The ions with m/z 309.1 and m/z 310.1, corresponding to the y2 fragment ions of **2-d-X** after incorporation of two or three deuterons, respectively, were fragmented. The MS³ spectra are displayed in Figure 3.

i) Fragmentation of the y2 fragment ion of 2-d-X after incorporation of two deuterons (m/z 309.1): The ion with m/z 309.1 was selected for MS³ fragmentation. It corresponds to the y2-fragment ion of **2-d** after incorporation of two deuterons during the reaction with AAPH in D₂O. The formation of the fragment ions with m/z 291.1, 262.1, and 203.1 (Fig. 3, A) is explained in the Supplementary Material, in section S1.1. The reaction mechanism is displayed in Scheme 2. This reaction mechanism is consistent with the incorporation of the second deuterium into product **2-d-Cys[^{13}C]** or **2-d-Cys[^{13}C]** (in Scheme 2, the fragmentation is representatively shown for the second deuterium covalently bound to the ^{13}C carbon of Cys, i.e. for **2-d-Cys[^{13}C]**).

ii) Fragmentation of the y2 fragment ion of 2-d-X after incorporation of three deuterons (m/z 310.1): The third deuterium can be incorporated either on the ^{13}C or ^{13}C carbons of the Cys residue or on the ^{13}C carbon of Gly*.

The ion with m/z 310.1 was selected for MS³ fragmentation. It corresponds to the y2-fragment ion of **2-d-X** after incorporation of three deuterons during the reaction with AAPH in D₂O. The formation of the fragment ions with m/z 292.1, 263.1, 203.1, and 204.1 (Fig. 3, B) is explained in the Supplementary Material, in section S1.2. The reaction mechanism is displayed in Scheme 2. The presence of the ion with m/z 204.1 (Fig. 3, insert B1) provides evidence that the third deuterium is also incorporated into Cys (rather than Gly*), either on the ^{13}C or the ^{13}C carbon. The concomitant observation of the ion with m/z 215.1 (Fig. 3, insert B2) suggests that both ^{13}C and ^{13}C of Cys contain one deuterium each. In such case, the fragmentation pathway is fully explained through reactions 18b-21b, invoking the same neutral losses as described in reactions 14– 17 (Scheme 2). In summary, the MS² analysis of **2-d-X** provides strong evidence for covalent H/D exchange at ^{13}C and ^{13}C of Cys.

MS³ analysis of product 3-d-X—After reaction of GSH* with AAPH in H₂O and D₂O and subsequent derivatization of GSH* with IOA, a comparison of the MS¹ spectra of products **3-h** (m/z 368.1) and **3-d-X** (m/z 371.1) indicate the incorporation of three deuterons into product **3-d-X**. To localize the deuterium atoms in **3-d-X**, an MS³ analysis of the y2 fragment ion was performed. The ions with m/z 239.1 and 242.1 correspond to the y2 fragment ions of **3-h** and **3-d-X**, respectively, after incorporation of three deuterons. The MS³ spectra are displayed in Figure 4. The derivatization of Cys with IOA in D₂O does not require any deuterium incorporation into the acetamide group. Therefore, the three deuterons incorporated into product **3-d-X** are located on the ^{13}C carbon of Gly and/or the ^{13}C and/

or ^{13}C carbons of Cys. In order to locate the deuterons we have compared the y_2 fragments of **3-h** and **3-d-X**, after incorporation of three deuterons into **3-d-X**.

i) Fragmentation of the y_2 fragment ion of 3-h (no deuterium incorporated): The ion with m/z 239.1 was selected for MS^3 fragmentation. It corresponds to the y_2 fragment ion of **3-h**. The fragmentation spectrum is displayed in Figure 4, A. The fragmentation mechanism is given in Scheme 3, with $\text{X}^1=\text{X}^2=\text{X}^3=\text{X}^4=\text{H}$. The ions with m/z 220.9, 194.0, and 148.0 are rationalized in section S2 of the Supplementary Material.

ii) Fragmentation of the y_2 fragment ion of 3-d-X after incorporation of three deuterons (m/z 242.1): The ion with m/z 242.1 was selected for MS^3 fragmentation. It corresponds to the y_2 fragment ion of **3-d-X**. The fragmentation spectrum is displayed in Figure 4, B, and the fragmentation mechanism is given in Scheme 3. The fragmentation mechanism is similar to the one described above for the y_2 fragment of **3-h**. Three deuterons are located on the y_2 fragment ion of product **3-d-X**. These deuterons can occupy three of the positions X^1 , X^2 , X^3 , or X^4 , as outlined in Scheme 3. The smallest fragment detected is the ion with m/z 133.0. Such ion results from the loss of H_2O from the ion with m/z 151.0 (Scheme 3, reactions 28–30). The fragmentation mechanism leading to the formation of the ion with m/z 151.0 involves reaction 27. Due to the low amount of material, none of the ions resulting from the further loss of ^{13}CO and $^{15}\text{NH}=\text{C}^{13}\text{H}$ are observed. Consequently, the MS^3 fragmentation of trideuterated y_2 cannot give any further information on whether deuterium is incorporated in Gly*. Nevertheless, the presence of three deuterons in y_2 of **3-d-X** confirms that at least one deuterium must be located on the Cys residue.

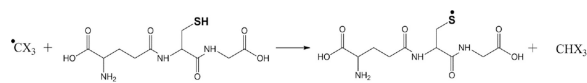
3.3 UV-irradiation of GSSG

UV-irradiation ($\lambda = 253.7$ nm) of GSSG leads to the formation of GSH *via* an initial pair of GS^{\bullet} . The isotopic distributions of GSH generated in H_2O and D_2O , respectively, and derivatized with NEM (products **2-h** and **2-d-X**) are compared in Figure 5. LC-MS analysis reveals that product **2-d-X** has incorporated deuterons. The respective percentages of **2-d-X** which have incorporated one and two deuterons increase over a pH/pD range of 7.1–9.1 (Fig. 5, inserted table).

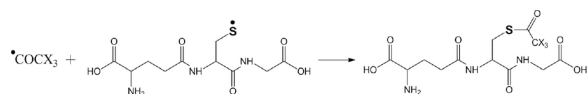
3.4 Photochemistry of acetone in the presence of GSH and GS^{\bullet} : analysis of the b_2 ion

The 253.7 nm photolysis of acetone at room temperature leads to the formation of methyl ($\text{H}_3\text{C}^{\bullet}$) and acetyl radicals ($\text{CH}_3\text{C}^{\bullet}\text{O}$).³⁷ These radicals are able to abstract an H-atom from GSH³⁸ to yield GS^{\bullet} which subsequently enters reversible H-transfer reactions (Scheme 1, reactions 11–13). More details about the photochemistry of sulfur-containing peptides in the presence of acetone are given elsewhere.²⁹ Ultimately, both $\text{H}_3\text{C}^{\bullet}$ and $\text{CH}_3\text{C}^{\bullet}\text{O}$ can combine either with C- and S-centered radicals of GSH and GS^{\bullet} . Specifically, the recombination products with carbon-centered radicals of GSH and GS^{\bullet} provide information about the original formation and location of intermediary carbon-centered radicals. Hence, the recombination products were analysed by mass spectrometry.

i) Acetylation of the thiol—Products **4-h-S** (m/z 350.1, $\text{CH}_3\text{C}(\text{O})\text{-SG}$, Table 4) and **4-d-S** (m/z 353.1, $\text{CD}_3\text{C}(\text{O})\text{-SG}$, Table 4) are the results of the acetylation of the thiol function during the photolysis of acetone- h_6 and acetone- d_6 , respectively, in the presence of GSH (reactions 31 and 32, X stands for H or D, depending on the use of acetone- h_6 or acetone- d_6).



(31)



(32)

The acetylation of Cys in GSH is demonstrated through MS³ analysis of the b2 fragment ions of products **4-h-S** and **4-d-S**, displayed in Figures 6A and 6B, where **4-h-S** and **4-d-S** display m/z 275.1 and m/z 278.1, respectively.

The b2 fragment ion is an amino-acylium ion that cyclizes through reaction 33 (Scheme 4, **I₁**). This cyclic intermediate (**I₁**) is used to explain the formation of all fragment ions observed during MS³ fragmentation of the b2 ions of products **4-h-S** and **4-d-S** (Figure 6, A and B). The structure of **I₁** was confirmed independently by MS⁴ analysis (see below). The fragmentation pathway of the b2 ions of **4-h-S** and **4-d-S** is explained in the Supplementary Material, section S3. The fragmentation mechanisms are displayed in Scheme 4 and 5.

To confirm the structure of **I₁**, we have further fragmented the ion with m/z 199 (Figure 6, C). The formation of ions with m/z 181.0, 153.0, and 135.0 during MS⁴ is explained in section S4 of the Supplementary Material. The formation of the cyclic intermediate **I₁** is also supported by calculations presented in the Supplementary Material (Scheme S1). The calculations show that the intermediate **I₁** is more stable than the b2 ion by 23.63 kcal/mol. The activation in the gas-phase of intermediate **I₁** allows further fragmentation of the b2 ion. Because the loss from **I₁** of the ketene group is more favourable than the loss of H₂O (See calculations in Supplementary Material, Scheme S1), we believe that the fragmentation pathways described in Scheme 5 are more likely to occur than those described in Scheme 4.

ii) Acetylation of the γ Glu residue—The presence of ions with m/z 172.0 (Fig. 6, A) and m/z 175.0 (Fig. 6, B) suggest also that the γ Glu residue of GSH is acetylated during the photolysis of GSH in the presence of acetone-h₆ (and acetone-d₆). The low intensity of these ions did not allow further fragmentation to localize with more precision the acetylation site within γ Glu.

3.5 Photochemistry of acetone in the presence of GSH and GSH*: analysis of the y2 ion

The acetylation of Cys and Gly/Gly* will be analyzed through fragmentation pathways of the y2 fragment ions of products **4-h-S**, **4-d-S**, **5-h-Y**, **5-d-Y**, **6-h-S** and **7-h-Y** (Table 4). Here, the labels **h** and **d** refer to the use of acetone-h₆ and acetone-d₆, respectively. The label **S** refers to the acetylation of the thiol group. The label **Y** summarizes an acetylation on either the α C carbon of Cys, the α C carbon of Gly or the β C carbon of Cys. When we will refer to one of these products, the **Y** label will be replaced with either the label **Cys[α C]**, **Gly[α C]** (or **Gly[α C¹³]**, in GSH*), or **Cys[β C]**.

In summary, products **4-h-S**, **5-h-Y**, **6-h-S**, and **7-h-Y** correspond to the acetylation products of GSH during the photolysis of acetone-h₆. Products **4-d-S**, and **5-d-Y** correspond to the acetylation products of GSH during the photolysis of acetone-d₆. The mechanism leading to

the formation of **4-h-S** and **4-d-S** is described in reactions 31 and 32 (see above). The formation of products **5-h-Y** and **5-d-Y** is explained through reactions 56 to 58 (Scheme 6). The mechanism leading to the formation of **6-h-S** proceeds through reactions 31 and 32 (see above, the reactions are representatively shown only for GSH). The formation of products **7-h-Y** is explained by reactions 59 to 61 (Scheme 6).

The MS³ spectra of the y₂ fragments ions are displayed in Figure 7.

i) Acetylation of the thiol—The acetylation of the sulfhydryl group during the photolysis of acetone in the presence of GSH and GSH* is confirmed by the analysis of the y₂ fragment ions of the products **4-h-S** (m/z 221.0), **4-d-S** (m/z 224.0) and **6-h-S** (m/z 224.0) (Figure 7, A, B and C). To follow the fragmentation routes of the ions, the y₂ ions and their fragments derived from **4-h-S**, **4-d-S** and **6-h-S** are colored in black, blue and red, respectively, and presented in Scheme 7.

During MS analysis, products **4-h-S** and **6-h-S** generate y₂ ions with m/z 221.0 and 224.0, respectively (Scheme 7, Figure 7, A, C). The reactions explaining the proton migration occurring during the fragmentation of the y₂ ions are given in the Supplementary Material, in section S5.

The photo-irradiation of GSH in the presence of acetone-d₆ yields product **4-d-S**. During MS analysis, product **4-d-S** generates the y₂ ion with m/z 224.0 (Scheme 7, blue, Fig. 7, B). The fragmentation of this y₂ ion according to reactions 62b-64b (Scheme 7) generates I₂ with m/z 162.0. Reaction 64b (Scheme 7), cleaving off the deuterated acetamide (NH²COCD₃), supports the mechanism depicted in Scheme 7 and is mechanistically described in the Supplementary Material (section S5).

ii) Acetylation of Gly[^αC]—The products **5-h-Gly[^αC]**, **5-d-Gly[^αC]**, **7-h-Gly[^αC]** arise from the recombination of CH₃C*O with a carbon-centered radical on Gly/Gly*, and can be analyzed through further fragmentation of the y₂ ion. In fact, it will be shown that only the acylation of Gly/Gly* can fully explain the nature of the fragment ions derived from y₂. Our proposed reaction schemes for the fragmentation of the y₂ ions of the products **5-h-Cys[^αC]**, **5-h-Cys[^βC]**, **5-d-Cys[^αC]**, **5-d-Cys[^βC]**, **7-h-Cys[^αC]**, and **7-h-Cys[^βC]** (Table 4) are presented in Scheme 8 and in the Supplementary Material (Schemes S1 and S2).

During MS² fragmentation the products **5-h-Gly[^αC]**, **5-d-Gly[^αC]**, **7-h-Gly[^αC]** generate the y₂ fragments ions with m/z 221.0, 224.0, and 224.0, respectively. These ions were selected for MS³ analysis (Figure 7, A, B, C, and Scheme 8). The m/z of the fragment ions resulting from the collision-induced dissociation of the y₂ ions of **5-h-Gly[^αC]**, **5-d-Gly[^αC]**, and **7-h-Gly[^αC]** are displayed in black, blue and red, respectively (Scheme 8). The initial fragmentation (Scheme 8, reactions 68–73) of the y₂ ions of the three products **5-h-Gly[^αC]**, **5-d-Gly[^αC]**, **7-h-Gly[^αC]** is similar. After proton transfer from the N-terminal amine to the ketone function, the N-terminal amine cyclizes to a six-membered ring (Scheme 8, reaction 68). The subsequent proton transfer reactions allowing for the description of the fragmentation profile of the y₂ ions (Figure 7) are detailed in the Supplementary Material, in section S6.

iii) Acetylation of Cys[^αC] or Cys[^βC]—The products **5-h-Cys[^αC]** and **5-h-Cys[^βC]** are isobaric to the product **5-h-Gly[^αC]**, the products **5-d-Cys[^αC]** and **5-d-Cys[^βC]** are isobaric to the product **5-d-Gly[^αC]**, and the products **7-h-Cys[^αC]** and **7-h-Cys[^βC]** are isobaric to the product **7-h-Gly[^αC]**. Thus, during the fragmentation of the y₂ ions of products **5-h-Gly[^αC]**, **5-d-Gly[^αC]** and **7-h-Gly[^αC]** some of the fragment ions (Fig. 7, A,

B, C) could be related to the fragmentation of the y₂ ions of products **5-h-Cys**[^αC], **5-h-Cys**[^βC], **5-d-Cys**[^αC], **5-d-Cys**[^βC], **7-h-Cys**[^αC] and **7-h-Cys**[^βC].

In the following, we demonstrate that the acetylation of the Cys[^αC] or Cys[^βC] positions are less likely.

a) The acetylation of Cys[^αC]: The fragmentation mechanism of the hypothetical y₂ ions of products **5-h-Cys**[^αC], **5-d-Cys**[^αC], and **7-h-Cys**[^αC] can start with a cyclization between the thiol and the ketone as describe in reaction 81 (Scheme S2). Such cyclization allows for the loss of a first molecule of H₂O (Scheme S2, reactions 82–83) and the formation of the ions with m/z 203.0, 206.0 and 206.0 (Fig. 7, A, B, C). Subsequently, the loss of ¹²CO (MW = 28 Da) or ¹³CO (MW = 29 Da) through reaction 84 (Scheme S2), and the loss of the imine group (Scheme S2, reaction 85) could yield ions with m/z 175.0, 178.0, and 177.0, and 146.0, 149.0, and 146.0, respectively. However, such combinations of ions are not observed. Other potential cyclizations were tested but none of them could explain the entire fragmentation pattern presented in Figure 7 (A, B, C).

b) The acetylation of Cys[^βC]: The acetylation of Cys[^βC] appears sterically more probable than the acetylation of Cys[^αC]. In order to match as many fragments ions as possible observed during the fragmentation of the hypothetical y₂ ions of products **5-h-Cys**[^βC], **5-d-Cys**[^βC], and **7-h-Cys**[^βC], the fragmentation mechanism must start with a cyclization between the nitrogen of the amide bond and the ketone as describe in reaction 87 (Scheme S3). The mobile proton on the nitrogen can be used to protonate the alcohol function to allow the loss of the first molecule of H₂O (Scheme S3, reactions 88–89) and the formation of a new set of ions with m/z 203.0, 206.0 and 206.0 (Figure 7, A, B, C). The carbocation resulting from the loss of the first molecule of H₂O, can be used to cyclize the primary amine (Scheme S2, reaction 90). Such cyclization would permit the formation of a mobile proton that could be used to protonate the carboxylic acid function to allow the loss of the second molecule of H₂O (Scheme S3, reactions 91–92). The second loss of H₂O permits the formation of a set of ions with m/z 185.0, 188.0, and 188.0, as observed in Figure 7 (A, B, C). The subsequent loss of ¹²CO (MW = 28 Da) or ¹³CO (MW = 29 Da) (Scheme S3, reaction 93) can explain the formation of the set of ions with m/z 157.0, 160.0, and 159.0, respectively. However, we cannot rationalize further fragmentations from these set of ions to yield new fragments with m/z 128.0, 131.0, and 128.0 and m/z 100.0, 103.0, and 100.0, respectively. These latter ions can only be rationalized by acetylation on Gly[^αC] (See above, Scheme 8).

iv) Acetylation of Cys[^αC], Cys[^βC] or Gly[^αC]: **Ab initio calculation of the Gibbs energies of the y₂ ions of products 5-h-Cys**[^αC], **5-h-Cys**[^βC], **5-h-Gly**[^αC]—The recombination of the acetyl radical (CH₃C[•]O) with a carbon-centered radical on Cys[^αC], Cys[^βC] or Gly[^αC] leads to the formation of new chiral carbons. During mass spectrometry analysis, the formation of the y₂ fragment ions of **5-h-Cys**[^αC], **5-h-Cys**[^βC] and **5-h-Gly**[^αC] generates cyclic ions which lead to further fragmentation. Our analysis of MS³ and MS⁴ spectra show that the only way to fully rationalize the formation of all fragment ions of the y₂ ions is to start the fragmentation from the six-membered ring generated from y₂ of **5-h-Gly**[^αC] (Table 5, Scheme 8). Our calculations show that for all the combinations of absolute configurations of the cyclic y₂ ions presented in Table 5, the most stable configuration under vacuum is the hexacyclic ion obtained from product **5-h-Gly**[^αC] (if the absolute configuration is (S,R,R)). Thus, these calculations provide additional support for the formation of such ions in the gas phase and support our proposed fragmentation mechanisms suggesting the acetylation of Gly[^αC].

3.6 Formation of dehydroalanine during the reaction of GSH with AAPH

The exposure of GSH to AAPH generates a glutathione-thioether (GSG, m/z 581.2), corresponding to the formal loss of one sulfur atom from GSSG. The isotopic distribution is given in the Supplementary Material (Figure S1). The formation of the thioether is rationalized by the transformation of Cys into dehydroalanine, followed by the addition of the thiol of a second molecule of GSH (Scheme S4). The transformation of Cys into dehydroalanine (Dha) results from a 1,3-H-transfer between the sulfur-centered radical and the α C-H bond of Cys.³² The formation of such product further supports the formation of a carbon-centered radical through intramolecular hydrogen transfer reactions of GS \cdot .

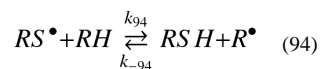
4. Discussion

Earlier experimental^{13,17,18} and computational²⁴ studies supported an intramolecular hydrogen transfer reaction between the thiyl radical GS \cdot and the α C-H bond of the γ -glutamyl moiety of glutathione. The bond dissociation enthalpies (BDE) of the different α C-H bonds in GSH, based on the method of isodesmic reactions, decrease in the following order: α C-H (Cys): 346 kJ mol⁻¹, α C-H (Gly): 344 kJ mol⁻¹, and α C-H (Gln): 320 kJ mol⁻¹.^{24,39} The low BDE of α C-H (Gln) is consistent with the experimental observation of the formation of an α C-centered radical at the Gln moiety.¹⁸ On the other hand, the calculated free energy of activation for the H-atom transfer reaction between GS \cdot and the α C-H bond at Gly is hindered by a barrier of 134 kJ mol⁻¹.²⁴

Here, we provide evidence for additional *intramolecular* hydrogen transfer reactions in GS \cdot , namely reversible hydrogen transfer between the thiyl radical in GS \cdot and (i) the C-terminal Gly (or Gly*) residue, and (ii) the α C-H and β C-H bonds in Cys itself. The latter reactions correspond to 1,3- and 1,2-H atom transfers of the Cys thiyl radical, CysS \cdot , in GS \cdot . We hypothesize that the formation of the C-centered radicals are the results of reversible hydrogen atom transfer reactions between GS \cdot and C-H bonds present in GSH. Recently, Nauser et al.²⁶ have provided pulse radiolysis data supporting a 1,2- and 1,3-H atom transfer reactions in thiyl radical of model compounds. These reactions are most likely solvent-assisted. A proton-coupled electron transfer (PCET) is, therefore, a possibility, but in this paper we cannot experimentally distinguish PCET from hydrogen atom transfer (HAT).

A brief statement to exclude any intermolecular H-atom abstraction reactions between C-H bonds, in GSH, and the C-centered radicals or GS \cdot , is required.

For intermolecular H-atom transfer reactions, the rate constants k_{94} and k_{-94} are estimated to be $k_{94} = 3 \times 10^3 - 3 \times 10^4 \text{ M}^{-1}\text{s}^{-1}$,^{7,9,11} and $k_{-94} = 10^7 - 10^8 \text{ M}^{-1}\text{s}^{-1}$,⁴⁰ respectively.



Thus, under our conditions, the pseudo-first order rate constant for an intermolecular H-atom abstraction reaction between GS \cdot and a C-H bond of GSH (k_{94}) would be on the order of 2.3 - 23 s⁻¹. In comparison, the rate constant for an intramolecular 1,2-H atom transfer within CysS \cdot is several orders of magnitude faster (ca. 10⁵ s⁻¹).²⁶ Therefore, an intermolecular hydrogen abstraction reaction between GS \cdot and any C-H bond should be kinetically negligible. The C-centered radicals generated from the thermolysis of AAPH should react with the thiol of GSH (k_{-94}) with a pseudo-first order rate constant of ca. $5 \times 10^3 - 8 \times 10^4 \text{ s}^{-1}$. Moreover, the rate constants for H-atom abstraction reactions between methyl radicals and an S-H bond (in a thiol) and a C-H bond in glycine (or glycine

anhydride) are $4.0\text{--}7.4 \times 10^7 \text{ M}^{-1} \text{ s}^{-1}$ and $1.2 \times 10^2 - 4 \times 10^4 \text{ M}^{-1} \text{ s}^{-1}$, respectively, i.e. different by about three orders of magnitude.^{38,41,42} Assuming that AAPH-derived carbon-centered radicals, AAPH[C•], react with C-H bonds and the S-H bond of GSH with rate constants on the order of 4×10^4 and $4 \times 10^7 \text{ M}^{-1} \text{ s}^{-1}$, we can calculate the expected yield of deuterium incorporation only through an initial reaction of AAPH[C•] with the GSH C-H bonds. At 37°C, AAPH[C•] radicals are generated with a rate of $\text{AAPH}[\text{C}^\bullet] = 1.36 \times 10^{-6} [\text{AAPH}] (\text{M s}^{-1})$.⁴³ Hence, a one hour exposure of 2 mM AAPH yields ca. 10 μM AAPH[C•], of which ca. 0.1% are expected to react with the C-H bonds in GSH. However, over one hour ca. 40% of GSH at an initial concentration of 750 μM incorporated deuterium (Figure 1), i.e. a significantly higher yield compared to that expected if deuterium incorporation were initiated via reaction of AAPH[C•] with the C-H bonds of GSH. In fact, the yield is significantly higher than the initial yields of AAPH[C•], pointing to a chain reaction, which may be propagated through the reaction of a thiol radical with thiol, transferring the thyl radical from an already deuterated GSH to a non-deuterated GSH. The reaction of C-centered radicals with the C-H bonds can therefore be neglected. We also discussed, and demonstrated experimentally, that neither $\text{H}_3\text{C}^\bullet$ nor $\text{CH}_3\text{C}^\bullet\text{O}$ radicals, resulting from the photolysis of acetone, could efficiently abstract hydrogen atoms from $^\alpha\text{C}$ -H bonds in a model peptide, which did not contain Cys:²⁹ experimentally, we could neither observe product formation nor deuterium incorporation during the photolysis of hexaglycine in the presence of acetone.²⁹ Thus, the C-centered radicals resulting from i) the thermolysis of AAPH (AAPH[C•]), or ii) the photolysis of acetone ($\text{H}_3\text{C}^\bullet$, $\text{CH}_3\text{C}^\bullet\text{O}$) are more likely to react with the thiol moiety of GSH than with any C-H bond in GSH. We can, therefore, consider that any intermolecular hydrogen atom abstraction reaction either between GS^\bullet and a C-H bond or AAPH[C•] and a C-H bond would be largely negligible. Moreover, when GSSG was photolyzed, we observed deuterium incorporation into the final product, GSH-NEM. Especially for low turnovers ($0.1 < [\text{GSH}]/[\text{GSSG}] < 0.3$) an intermolecular H-atom transfer from the product GSH is kinetically unfavorable compared to that from the reactant GSSG, which is initially present at much higher concentration. Nauser et al.²⁶ also showed specifically for the 1,2-H atom transfer in thyl radicals from cysteamine, that the reaction is concentration-independent, i.e. intramolecular. All these experimental observations and kinetic data support the notion that intramolecular hydrogen atom transfer reactions are more favorable than intermolecular reactions under our experimental conditions.

The formation of a C-centered radical at Gly[$^\alpha\text{C}$] was demonstrated through the observation of deuterium incorporation at the Gly[$^\alpha\text{C}$] position, but also through the recombination of $\text{CH}_3\text{C}^\bullet\text{O}$ with Gly[$^\alpha\text{C}^\bullet$]. Indeed, when GS^\bullet radicals were generated through photolysis of acetone-containing solutions of GSH, recombination products of $\text{CH}_3\text{C}^\bullet\text{O}$ with radicals from GSH were detected. Specifically the recombination products **5-h-Gly[$^\alpha\text{C}$]**, **5-d-Gly[$^\alpha\text{C}$]** and **7-h-Gly[$^\alpha\text{C}$]** provide evidence for the recombination of $\text{CH}_3\text{C}^\bullet\text{O}$ with a carbon-centered radical of the Gly/Gly* residue, generated through intramolecular hydrogen abstraction from Gly/Gly* by the thyl radical of GS^\bullet .

The occurrence of 1,2- and 1,3-H atom transfers in Cys is specifically evident from the presence of up to three deuterons in the y2 fragments of products **2-d-X** and **3-d-X** as a result of GS^\bullet radical formation in D_2O . Here, MS^3 fragmentation of the y2 fragment of product **2-d-X** clearly provides evidence for the incorporation of up to a total of two deuterons into the original C-H bonds of $^\alpha\text{C}$ and $^\beta\text{C}$ of the Cys residue. Based on the structure of the Cys residue, these results demonstrate that at least one deuteron must be incorporated into the $^\beta\text{C}$ -H bond. The MS^3 fragmentation of the y2 fragment of product **3-d-X** provides additional evidence for the incorporation of deuterium into the Cys residue.

Specifically the 1,2-H atom transfer, depicted in reaction 56 in Scheme 6, leads to an α -mercaptoalkyl radical, $\text{R-C}^\bullet\text{H-SH}$. Based on theoretical calculations for 1,2-H atom transfer

equilibria of small organic radicals, such as $\text{CH}_3\text{S}^\bullet$ ⁴⁴ and $\text{HOCH}_2\text{CH}_2\text{S}^\bullet$,⁴⁵ we can expect that equilibrium 56 is located far on the side of the thiyl radical. For Cys with a polypeptide sequence, theoretical calculations provide homolytic bond dissociation energies at 298 K of 380.9 and 367.0 kJ/mol for the $\beta\text{C-H}$ and the S-H bonds, respectively, corresponding to a difference of ca. 13.9 kJ/mol.⁴⁶ These calculations suggest that in equilibrium 56, ca. 0.4% of the radicals may be present as α -mercaptoalkyl radicals. On the other hand, recent pulse radiolysis experiments on thiyl radicals from Cys and related model compounds suggest, that in aqueous solution a significant fraction of these thiyl radicals undergo a 1,2-H atom transfer.²⁶ Generally, activation energies for 1,2-H- and 1,3-H-shifts are high.⁴⁷ On the other hand, detailed mechanistic studies with alkoxy radicals ($\text{RCH}_2\text{O}^\bullet \rightarrow \text{RC}^\bullet\text{HOH}$) demonstrate that 1,2-H atom transfer reactions may be assisted by protic solvents, suggesting that solvent effects may also play a role in 1,2-H atom transfer reactions of thiyl radicals.⁴⁸ Calculations for Cys $\alpha\text{C-H}$ and S-H bonds at 298 K provide homolytic bond dissociation energies of 345.5 and 367 kJ/mol, clearly demonstrating that a 1,3-H atom transfer should be thermodynamically feasible.

Based on a homolytic bond dissociation energy of 344 kJ/mol for Gly $\alpha\text{C-H}$,³⁹ also the hydrogen transfer from Gly to the thiyl radical of GS^\bullet appears thermodynamically feasible. However, conformational restraints must be taken into account. A very high barrier of 134 kJ/mol was calculated for the (Z)-conformation of GS^\bullet .²⁴ However, reversible 1,3-H atom transfer within GS^\bullet may convert the original L-Cys into D-Cys (such conversion was recently observed for αC radicals of Ala in small model peptides²⁹), suggesting that additional conformations of GS^\bullet may have to be considered for hydrogen transfer. Importantly, reversible hydrogen transfer reactions between Cys thiyl radicals and adjacent Gly residues, in positions n+1 and n+2, have been observed for a series of model peptides.²⁸

The use of MS^n experiments for the identification of deuterated sites

The important features used to identify the positions of covalently incorporated deuterons during the MS^n experiments are not the structure of the different intermediates, but the nature of the neutral losses. This is, the comparison of the different changes of masses observed for each of the MS^n experiments, which allowed to determine when deuterons were removed from the ion, and, therefore, included in the neutral loss. The structures of the ions presented in the different Schemes were designed to explain as clearly as possible how a specific neutral loss converts an ion into a successor ion. We understand that some of these structures might be speculative in the absence of calculations. Even though the structures displayed in Schemes 4 and 5 are not based on calculations, they are the result of logical deduction from the comparison of multiple experimental results (MS^n spectra). In an effort to rationalize these structures, we have performed representative calculations to justify the formation of the cyclic structure I_1 (Schemes 4 and 5). The results of the calculations are presented in the Supplementary Material (Scheme S1). The results show that the intermediate I_1 is about 23 kcal/mol more stable than the b2 ion and can be used for further fragmentation as described in Schemes 4 and 5. Moreover, the calculations indicate that the fragmentation pathways in Scheme 5 are likely to be more favorable than the ones given in Scheme 4, since the ion resulting from I_1 after the loss of the ketene is more stable than the ion obtained after the loss of H_2O (Scheme S1).

The observed hydrogen transfer reactions are of biological significance. First, the conversion of GS^\bullet into carbon-centered radicals may provide the possibility for an irreversible formation of peroxy radicals through reaction with molecular oxygen.⁴⁹ Second, especially after the 1,3-H atom transfer of GS^\bullet , the resulting αC^\bullet radical at the Cys residue can undergo β -elimination of HS^\bullet to yield dehydroalanine. This reaction has been characterized in some detail for thiyl radicals of small Cys-containing model peptides.³² In accordance with such reaction, we detected the formation of thioether-linked glutathione dimers after the exposure

of GSH to AAPH (see Section 3.6). These thioether-linked dimers are likely the result of dehydroalanine formation followed by a Michael-type addition of a second GSH molecule. In vivo, dehydroalanine-containing products of GSH cause irreversible glutathiolation of proteins such as observed during cataract formation in the human lens.⁵⁰

5. Conclusion

A detailed mass spectrometry study of the fragment ions of deuterated and derivatized GSH allows the detection of intramolecular H-atom transfer reactions between GS• and the ¹³C-H bond at Gly. Additionally, covalent H/D exchange, within Cys provides evidence for a 1,2- and 1,3-H atom transfers. The latter is of particular interest, since subsequent β-elimination from the C_α-centered radical at Cys can generate DHA. The transformation of Cys into DHA in GSH is a potential source of thioether crosslinks in proteins.

Supplementary Material

Refer to Web version on PubMed Central for supplementary material.

Acknowledgments

Funding Support

We gratefully acknowledge financial support from the NIH (P01AG12993).

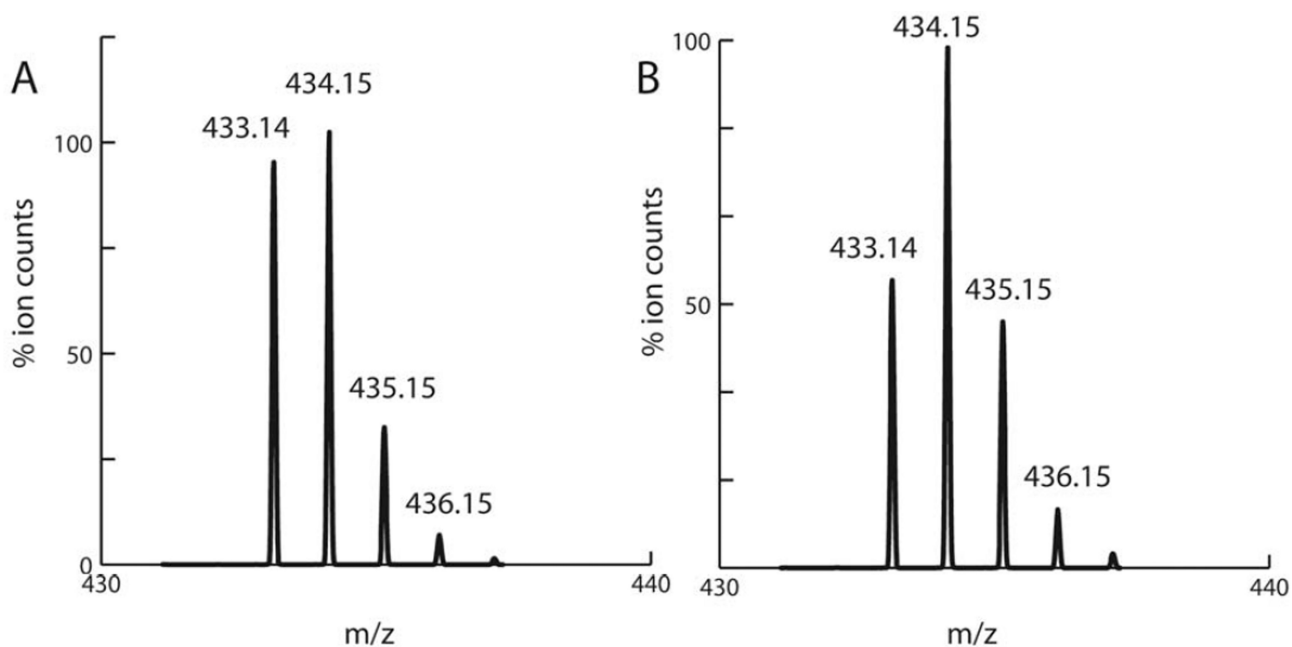
References

1. Fujii J, Ito J, Zhang XH, Kurahashi T. Unveiling the roles of the glutathione redox system in vivo by analyzing genetically modified mice. *J Clin Biochem Nutr.* 2011; 49:70–78. [PubMed: 21980221]
2. Tew KD, Manevich Y, Grek C, Xiong Y, Uys J, Townsend DM. The role of glutathione S-transferase P in signaling pathways and S-glutathionylation in cancer. *Free radical biology & medicine.* 2011; 51:299–313. [PubMed: 21558000]
3. Oakley A. Glutathione transferases: a structural perspective. *Drug Metab Rev.* 2011; 43:138–151. [PubMed: 21428697]
4. Gilbert HF. Thiol/Disulfide Exchange Equilibria and Disulfide Bond Stability. *Methods Enzymol.* 1995; 251:8–28. [PubMed: 7651233]
5. Ross D, Albano E, Nilsson U, Moldeus P. Thiyl Radicals - Formation during Peroxidase-Catalyzed Metabolism of Acetaminophen in the Presence of Thiols. *Biochem Biophys Res Commun.* 1984; 125:109–115. [PubMed: 6095833]
6. Von Sonntag, C. *The chemical basis of radiation biology.* London: Taylor & Francis; 1987.
7. Akhlaq MS, Schuchmann HP, von Sonntag C. The reverse of the 'repair' reaction of thiols: H-abstraction at carbon by thiyl radicals. *Int J Radiat Biol.* 1987; 51:91–102.
8. Schöneich C, Bonifati M, Asmus K. Reversible H-atom abstraction from alcohols by thiyl radicals: determination of absolute rate constants by pulse radiolysis. *Free Radic. Res. Commun.* 1989; 6:393–405. [PubMed: 2792850]
9. Schöneich C, Asmus K, Bonifati M. Determination of absolute rate constants for the reversible hydrogen-atom transfer between thiyl radicals and alcohols or ethers. *J. Chem. Soc. Faraday Trans.* 1995; 91:1923–1930.
10. Roberts BP. Understanding the rates of hydrogen-atom abstraction reactions: empirical, semi-empirical and ab initio approaches. *J. Chem. Soc. Perkin Trans.* 1996; 2:2719–2725.
11. Pogocki D, Schöneich C. Thiyl radicals abstract hydrogen atoms from carbohydrates: reactivity and selectivity. *Free Radic. Biol. Med.* 2001; 31:98–107. [PubMed: 11425495]
12. Schöneich C, Asmus KD, Dillinger U, Von Bruchhausen F. Thiyl Radical Attack on Poly-Unsaturated Fatty-Acids - a Possible Route to Lipid-Peroxidation. *Biochem Biophys Res Commun.* 1989; 161:113–120. [PubMed: 2567162]

13. Zhao R, Lind J, Merényi G, Eriksen TE. Kinetics of One-Electron Oxidation of Thiols and Hydrogen Abstraction by Thiyl Radicals from α -Amino C-H Bonds. *J. Am. Chem. Soc.* 1994; 116:12010–12015.
14. Nauser T, Schöneich C. Thiyl radicals abstract hydrogen atoms from the $^{\alpha}$ C-H bonds in model peptides: absolute rate constants and effect of amino acid structure. *J. Am. Chem. Soc.* 2003; 125:2042–2043. [PubMed: 12590520]
15. Nauser T, Casi G, Koppenol W, Schöneich C. Reversible Intramolecular Hydrogen Transfer between Cysteine Thiyl Radicals and Glycine and Alanine in Model Peptides: Absolute Rate Constants Derived from Pulse Radiolysis and Laser Flash Photolysis. *J. Phys. Chem. B.* 2008; 112:15034–15044. [PubMed: 18973367]
16. Raffy Q, Buisson DA, Cintrat JC, Rousseau B, Pin S, Renault JP. Carbon-centered radicals can transfer hydrogen atoms between amino acid side chains. *Angew Chem Int Ed Engl.* 2012; 51:2960–2963. [PubMed: 22311744]
17. Grierson L, Hildenbrand K, Bothe E. Intramolecular transformation reaction of the glutathione thiyl radical into a non-sulphur-centred radical: a pulse-radiolysis and EPR study. *International journal of radiation biology and related studies in physics, chemistry, and medicine.* 1992; 62:265–277.
18. Zhao R, Lind J, Merényi G, Eriksen TE. Significance of the intramolecular transformation of glutathione thiyl radicals to α -aminoalkyl radicals. *Thermochemical and biological implications.* *J. Chem. Soc. Perkin Trans.* 1997; 2:569–574.
19. Fessenden RW, Neta P. Electron Spin Resonance Study of Radicals Produced in Irradiated Aqueous Solutions of Thiols. *J. Phys. Chem.* 1971; 75:2277–2283.
20. Karoui H, Hogg N, Frejaville C, Tordo P, Kalyanaraman B. Characterization of sulfur-centered radical intermediates formed during the oxidation of thiols and sulfite by peroxydinitrite - ESR-SPIN trapping and oxygen uptake studies. *The Journal of biological chemistry.* 1996; 271:6000–6009. [PubMed: 8626383]
21. Hofstetter D, Nauser T, Koppenol WH. Hydrogen Exchange Equilibria in Glutathione Radicals: Rate Constants. *Chem. Res. Toxicol.* 2010; 23:1596–1600. [PubMed: 20882988]
22. Volman DH, Wolstenholme J, Hadley SG. Photochemical formation of free radical from hydrogen sulfide, mercaptans, and cysteine. *J. Phys. Chem.* 1967; 71:1798–1802. [PubMed: 4292576]
23. Skelton J, Adam FC. The Photolysis and Radiolysis of Simple Mercaptans in Dilute Glassy Matrices. *Can. J. Chem.* 1971; 49:3536–3543.
24. Rauk A, Armstrong DA, Berges J. Glutathione radical: intramolecular H abstraction by thiyl radical. *Can. J. Chem.* 2001; 79:405–417.
25. Osburn S, Berden G, Oomens J, O'Hair RAJ, Ryzhov V. Structure and Reactivity of the N-Acetyl-Cysteine Radical Cation and Anion: Does Radical Migration Occur? *J. Am. Soc. Mass Spectrom.* 2011; 22:1794–1803. [PubMed: 21952893]
26. Nauser T, Koppenol W, Schöneich C. Reversible Hydrogen Transfer Reactions in Thiyl Radicals From Cysteine and Related Molecules: Absolute Kinetics and Equilibrium Constants Determined by Pulse Radiolysis. *The Journal of Physical Chemistry. B.* 2012
27. Mozziconacci O, Williams T, Kerwin B, Schöneich C. Reversible intramolecular hydrogen transfer between protein cysteine thiyl radicals and $^{\alpha}$ C-H bonds in insulin: control of selectivity by secondary structure. *J. Phys. Chem. B.* 2008; 112:15921–15932. [PubMed: 19368019]
28. Mozziconacci O, Sharov V, Williams TD, Kerwin BA, Schöneich C. Peptide cysteine thiyl radicals abstract hydrogen atoms from surrounding amino acids: the photolysis of a cystine containing model peptide. *J. Phys. Chem. B.* 2008; 112:9250–9257. [PubMed: 18611046]
29. Mozziconacci O, Kerwin BA, Schöneich C. Reversible hydrogen transfer between cysteine thiyl radical and glycine and alanine in model peptides: covalent H/D exchange, radical-radical reactions, and L- to D-Ala conversion. *J. Phys. Chem. B.* 2010; 114:6751–6762. [PubMed: 20415493]
30. Mozziconacci O, Kerwin B, Schöneich C. Photolysis of an intrachain peptide disulfide bond: primary and secondary processes, formation of H₂S, and hydrogen transfer reactions. *J. Phys. Chem. B.* 2010; 114:3668–3688. [PubMed: 20178349]

31. Mozziconacci O, Haywood J, Gorman EM, Munson E, Schöneich C. Photolysis of Recombinant Human Insulin in the Solid State: Formation of a Dithiohemiacetal Product at the C-Terminal Disulfide Bond. *Pharm. Res.* 2012; 29:121–133. [PubMed: 21748537]
32. Mozziconacci O, Kerwin BA, Schöneich C. Reversible Hydrogen Transfer Reactions of Cysteine Thiyl Radicals in Peptides: the Conversion of Cysteine into Dehydroalanine and Alanine, and of Alanine into Dehydroalanine. *J. Phys. Chem. B.* 2011; 115:12287–12305. [PubMed: 21895001]
33. Younis IR, Elliott M, Peer CJ, Cooper AJL, Pinto JT, Konat GW, Kraszpolski M, Petros WP, Callery PS. Dehydroalanine Analog of Glutathione: An Electrophilic Busulfan Metabolite That Binds to Human Glutathione S-Transferase A1-1. *J. Pharmacol. Exp. Ther.* 2008; 327:770–776. [PubMed: 18791061]
34. Ikehata K, Duzhak TG, Galeva NA, Ji T, Koen YM, Hanzlik RP. Protein targets of reactive metabolites of thiobenzamide in rat liver in vivo. *Chem. Res. Toxicol.* 2008; 21:1432–1442. [PubMed: 18547066]
35. Fung YM, Kjeldsen F, Silivra OA, Chan TW, Zubarev RA. Facile disulfide bond cleavage in gaseous peptide and protein cations by ultraviolet photodissociation at 157 nm. *Angewandte Chemie (International ed.* 2005; 44:6399–6403.
36. Frisch, MJTGW.; Schlegel, HB.; Scuseria, GE.; Robb, MA.; Cheeseman, JR.; Montgomery, JA., Jr; Vreven, T.; Kudin, KN.; Burant, JC.; Millam, JM.; Iyengar, SS.; Tomasi, J.; Barone, V.; Mennucci, B.; Cossi, M.; Scalmani, G.; Rega, N.; Petersson, GA.; Nakatsuji, H.; Hada, M.; Ehara, M.; Toyota, K.; Fukuda, R.; Hasegawa, J.; Ishida, M.; Nakajima, T.; Honda, Y.; Kitao, O.; Nakai, H.; Klene, M.; Li, X.; Knox, JE.; Hratchian, HP.; Cross, JB.; Bakken, V.; Adamo, C.; Jaramillo, J.; Gomperts, R.; Stratmann, RE.; Yazyev, O.; Austin, AJ.; Cammi, R.; Pomelli, C.; Ochterski, JW.; Ayala, PY.; Morokuma, K.; Voth, GA.; Salvador, P.; Dannenberg, JJ.; Zakrzewski, VG.; Dapprich, S.; Daniels, AD.; Strain, MC.; Farkas, O.; Malick, DK.; Rabuck, AD.; Raghavachari, K.; Foresman, JB.; Ortiz, JV.; Cui, Q.; Baboul, AG.; Clifford, S.; Cioslowski, J.; Stefanov, BB.; Liu, G.; Liashenko, A.; Piskorz, P.; Komaromi, I.; Martin, RL.; Fox, DJ.; Keith, T.; Al-Laham, MA.; Peng, CY.; Nanayakkara, A.; Challacombe, M.; Gill, PMW.; Johnson, B.; Chen, W.; Wong, MW.; Gonzalez, C.; Pople, JA. Gaussian 03, Revision C.02. Wallingford CT: Gaussian, Inc; 2004.
37. Gandini A, Hackett PA. Electronic relaxation processes in acetone and 1,1,1-trifluoroacetone vapor and the gas phase recombination of the acetyl radical at 22°C. *J. Am. Chem. Soc.* 1977; 99:6195–6205.
38. Huston P, Espenson JH, Bakac A. Kinetics of formation and reactions of thiyl radicals in aqueous solution. *Inorg. Chem.* 1992; 31:720–722.
39. Rauk A, Yu D, Taylor J, Shustov GV, Block DA, Armstrong DA. Effects of structure on alpha C-H bond enthalpies of amino acid residues: relevance to H transfers in enzyme mechanisms and in protein oxidation. *Biochemistry.* 1999; 38:9089–9096. [PubMed: 10413483]
40. von Sonntag, C. Sulfur-Centered Reactive Intermediates in Chemistry and Biology. In: Chatgililoglu, C.; Asmus, K-D., editors. NATO-ASI SerA. Vol. Vol. 197. New York and London: Plenum; 1990. p. 359
41. Moger G, Dobis O. The reaction of free methyl radicals with glycine in aqueous solution. *Magy. Kem. Foly.* 1970; 76:328–332.
42. Reid DL, Armstrong DA, Rauk A, von Sonntag C. H-atom abstraction by thiyl radicals from peptides and cyclic dipeptides. A theoretical study of reaction rates. *Phys. Chem. Chem. Phys.* 2003; 5:3994–3999.
43. Niki, E. Methods in Enzymology. In: Lester Packer, ANG., editor. Free radical initiators as source of water- or lipid-soluble peroxy radicals. Vol. Vol. 186. Academic Press; 1990. p. 100-108.
44. Fossey J, Sorba J. HO and HS substituent effect on alkyl radicals: an ab-initio molecular orbital study. *J. Mol. Struct.* 1989; 186:305–319.
45. Naumov S, Von Sonntag C. UV/Vis absorption spectra of alkyl-, vinyl-, aryl- and thiylperoxy radicals and some related radicals in aqueous solution. A quantum-chemical study. *J. Phys. Org. Chem.* 2005; 18:586–594.
46. Rauk A, Yu D, Armstrong DA. Oxidative Damage to and by Cysteine in Proteins: An ab Initio Study of the Radical Structures, C-H, S-H, and C-C Bond Dissociation Energies, and Transition Structures for H Abstraction by Thiyl Radicals. *J. Am. Chem. Soc.* 1998; 120:8848–8855.

47. Viskolcz B, Lendvay G, Körtvélyesi T, Seres L. Intramolecular H Atom Transfer Reactions in Alkyl Radicals and the Ring Strain Energy in the Transition Structure. *J. Am. Chem. Soc.* 1996; 118:3006–3009.
48. Konya KG, Paul T, Lin S, Luszyk J, Ingold KU. Laser flash photolysis studies on the first superoxide thermal source. First direct measurements of the rates of solvent-assisted 1,2-hydrogen atom shifts and a proposed new mechanism for this unusual rearrangement. *J. Am. Chem. Soc.* 2000; 122:7518–7527.
49. Davies MJ. The oxidative environment and protein damage. *Biochim. Biophys. Acta.* 2005; 1703:93–109. [PubMed: 15680218]
50. Linetsky M, LeGrand RD. Glutathionylation of lens proteins through the formation of thioether bond. *Cell. Biochem.* 2005; 272:133–144.



	Percentage of deuterons covalently incorporated	
	No deuteron	1 deuteron
pH 7.1	59%	41%
pH 8.1	63%	37%
pH 9.1	60%	40%

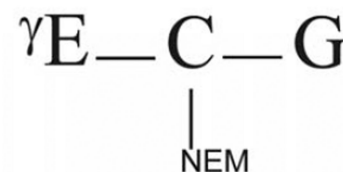


Figure 1.

MS spectra of GSH-NEM derivatized (m/z 433.14) obtained after exposure of GSH (500 μM) to AAPH (2 mM) at 37 $^{\circ}\text{C}$ during 1 hour in H_2O -buffer (A) and D_2O -buffer (B). The table summarizes the percentage of GSH-NEM derivatized molecules having incorporated covalently one deuterium atom after reaction of GSH with AAPH at different pH/pD in $\text{H}_2\text{O}/\text{D}_2\text{O}$ -buffers.

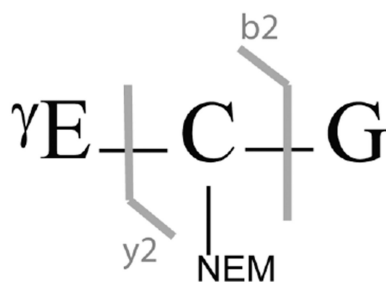
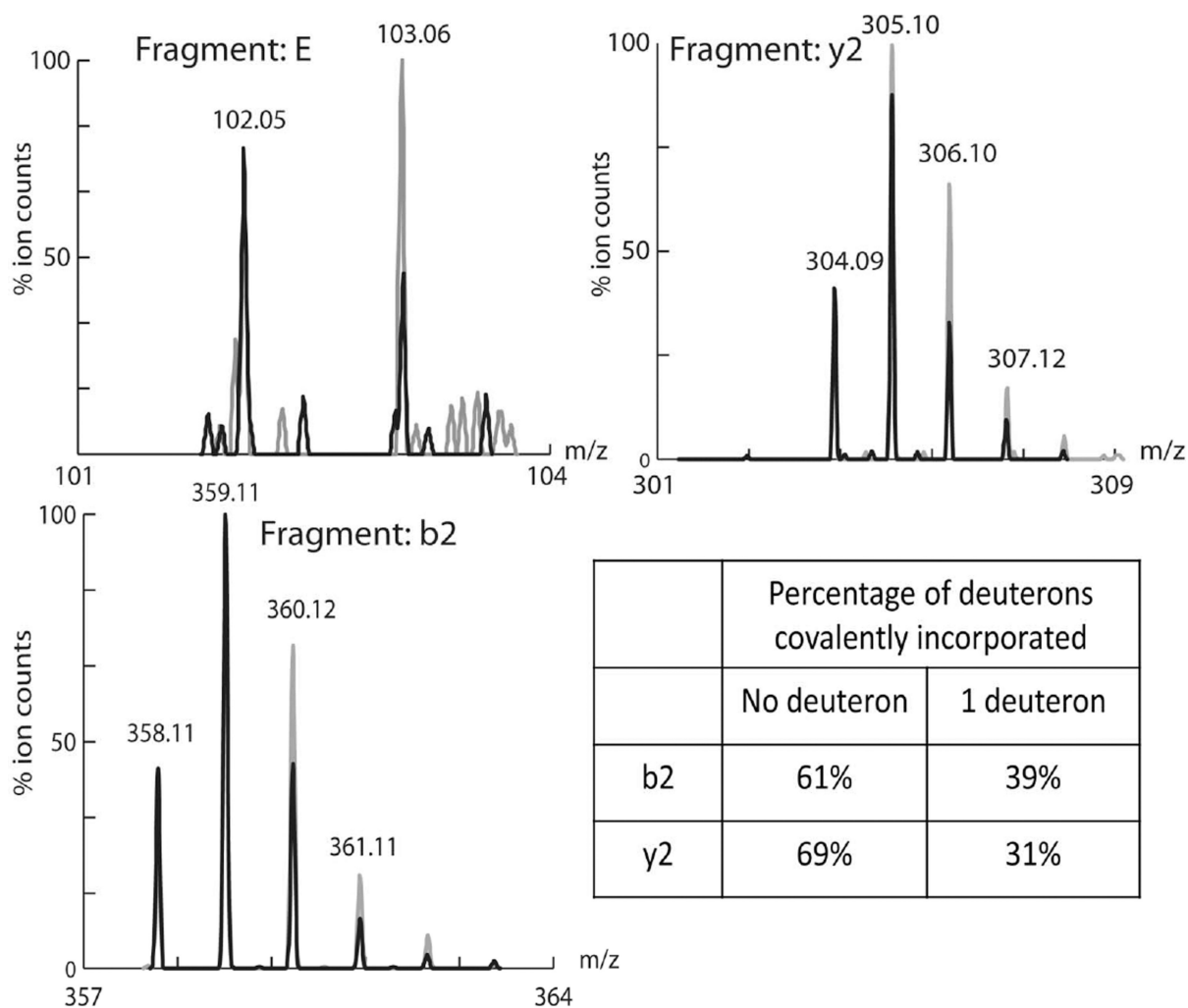


Figure 2.

Overlay of the CID spectra of GSH-NEM derivatized (m/z 433.14) obtained after exposure of GSH (500 μ M) to AAPH (2 mM) at 37 $^{\circ}$ C during 1 hour in H_2O -buffer (black) and D_2O -buffer (gray). The table summarizes the percentage of fragment ions having incorporated covalently one deuterium atom after reaction of GSH with AAPH at different pH/pD in H_2O/D_2O -buffers.

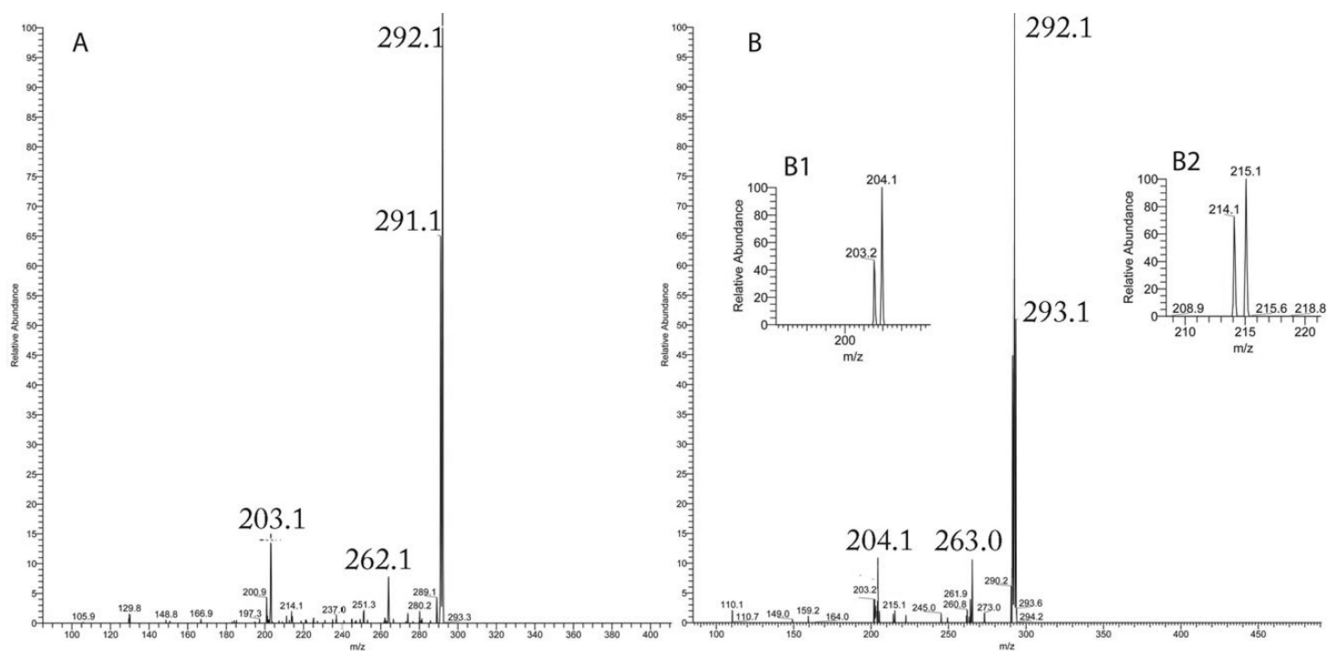


Figure 3. MS³ spectra of the y₂ fragment ions of product **2-d-X** after incorporation of A) two deuterons, B) three deuterons. **X** stands for deuterium incorporation at Cys[^αC], Cys[^βC], or Gly[^αC].

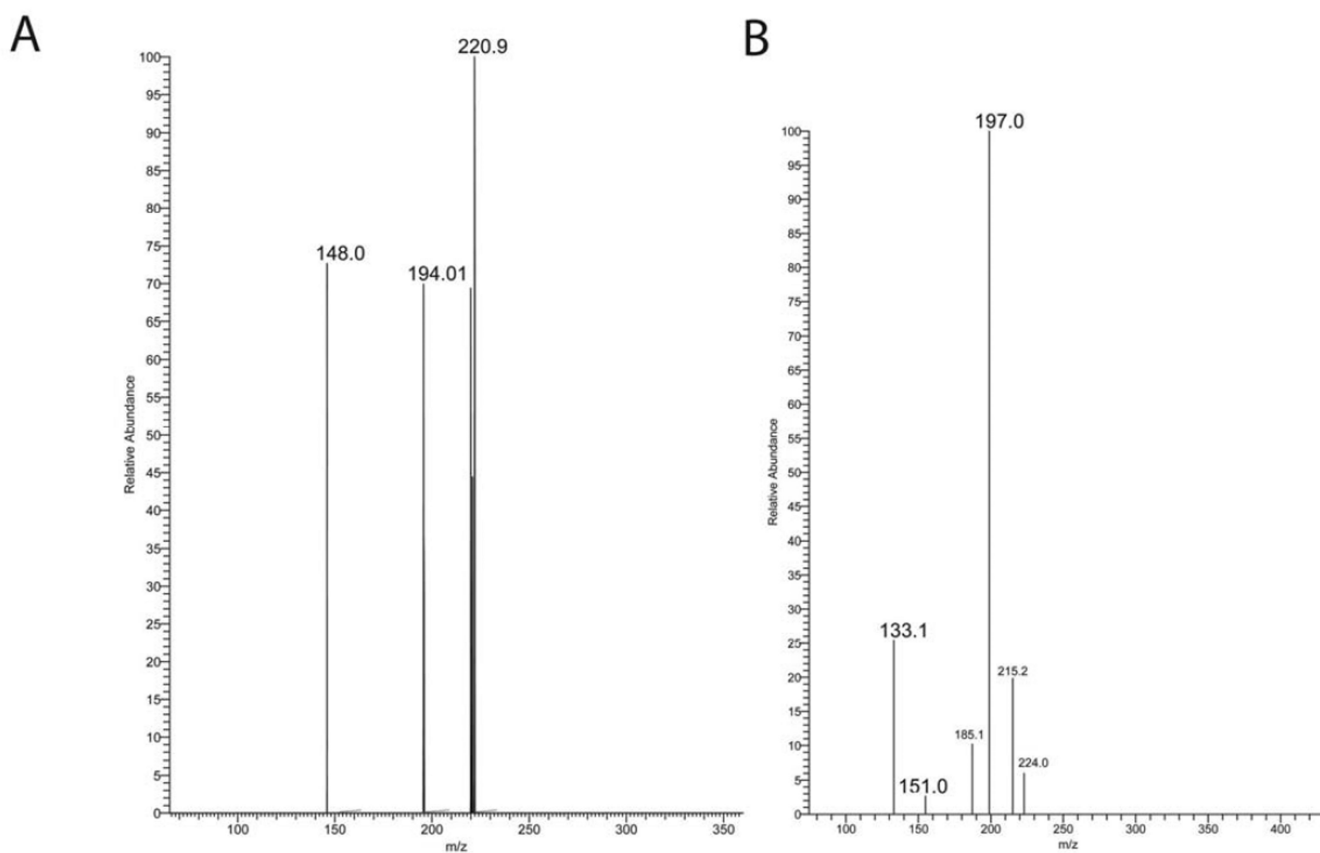
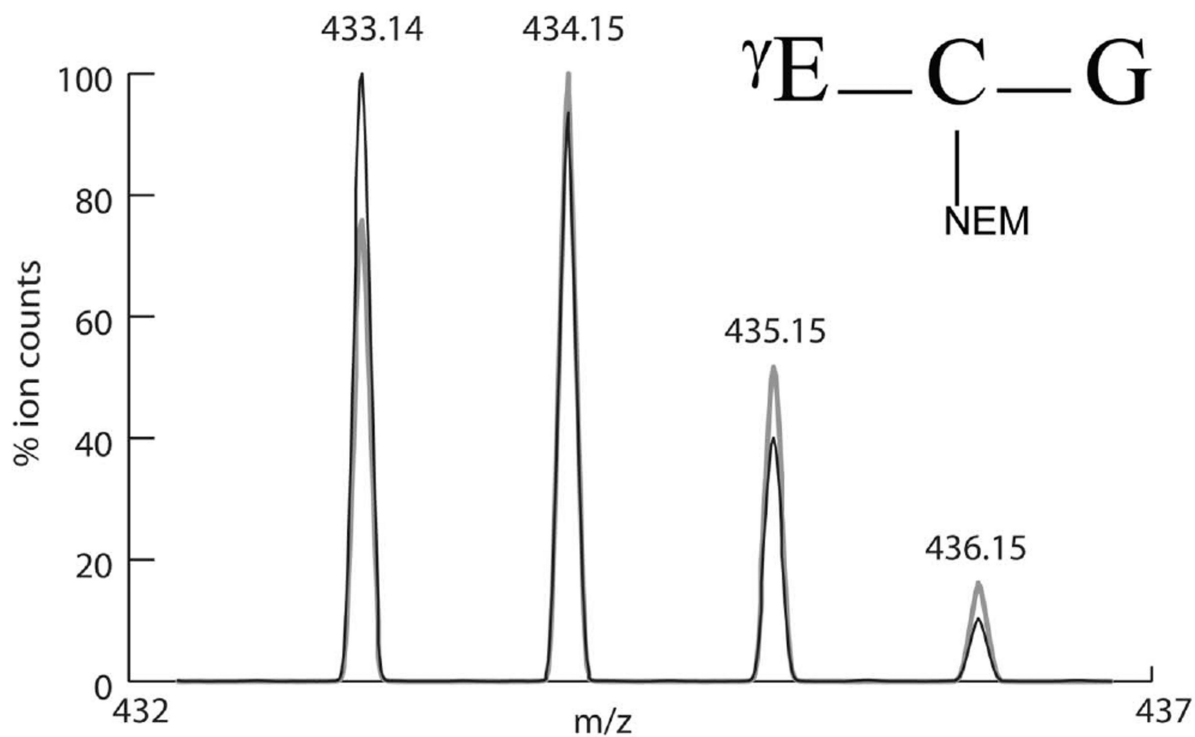


Figure 4. MS³ spectra of the y₂ fragment ions of A) product **3-h** and B) product **3-d-X** after incorporation of three deuterons. **X** stands for deuterium incorporation at Cys[^αC], Cys[^βC], or Gly[^αC].



	Percentage of deuterons covalently incorporated		
	No deuteron	1 deuteron	2 deuterons
pH 7.1	80%	20%	0%
pH 8.1	44%	50%	6%
pH 9.1	35%	54%	11%

Figure 5. Overlay of the MS spectra of **2-h** and **2-d-X** (m/z 433.14) generated after 10 min of UV-irradiation ($\lambda = 253.7$ nm) of GSSG (500 μM) in H_2O (black) and D_2O (gray). **X** stands for deuterium incorporation at **Cys**[$^{\alpha}\text{C}$], **Cys**[$^{\beta}\text{C}$], or **Gly**[$^{\alpha}\text{C}$].

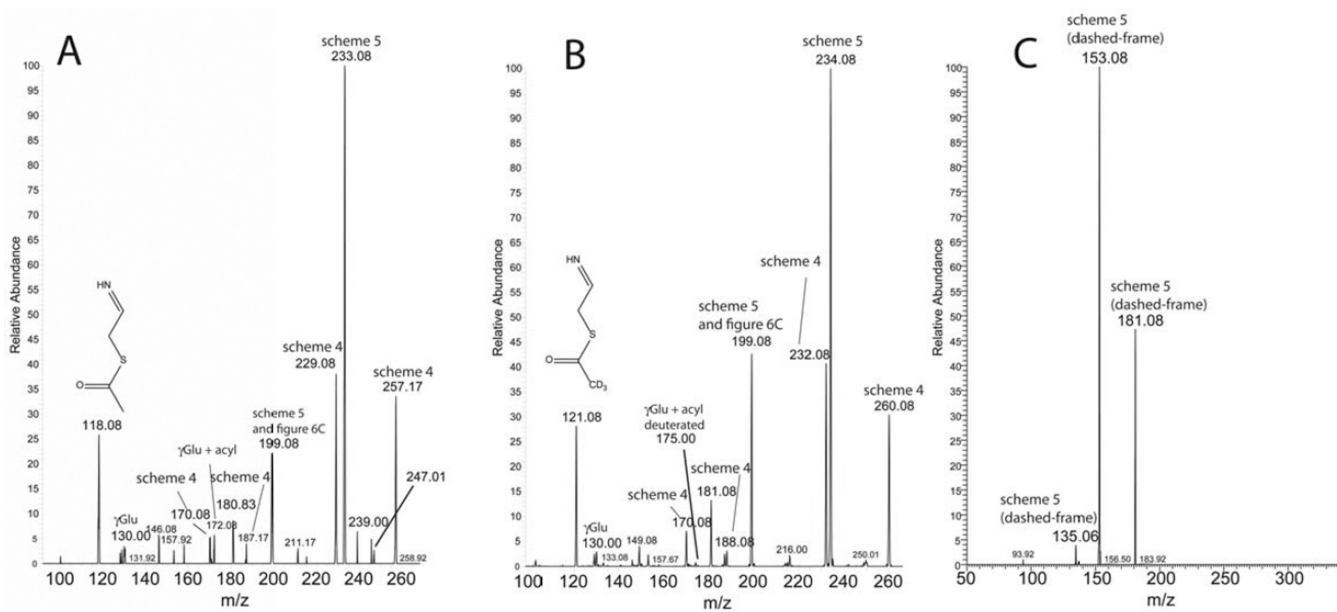


Figure 6. MS³ spectra of the b2 fragment ions of A) product **4-h-S** and B) product **4-d-S**. MS⁴ of the fragment ion with m/z 199.0 is presented in panel C.

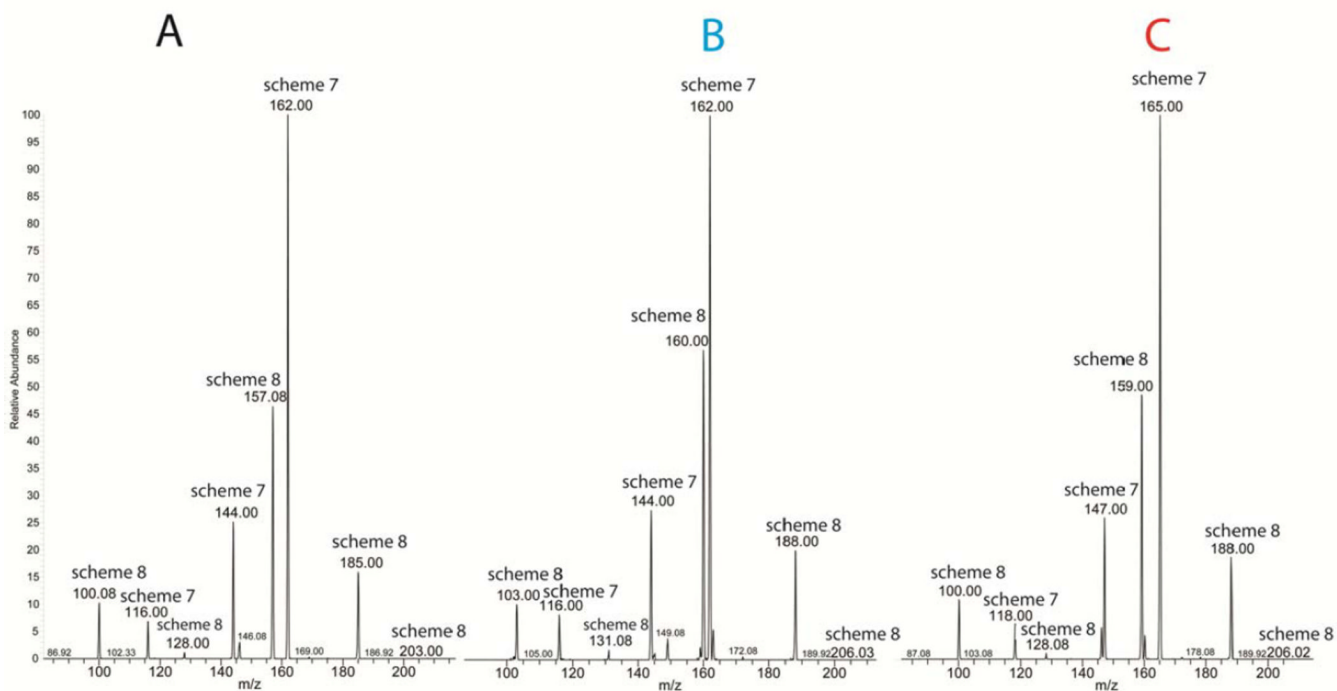
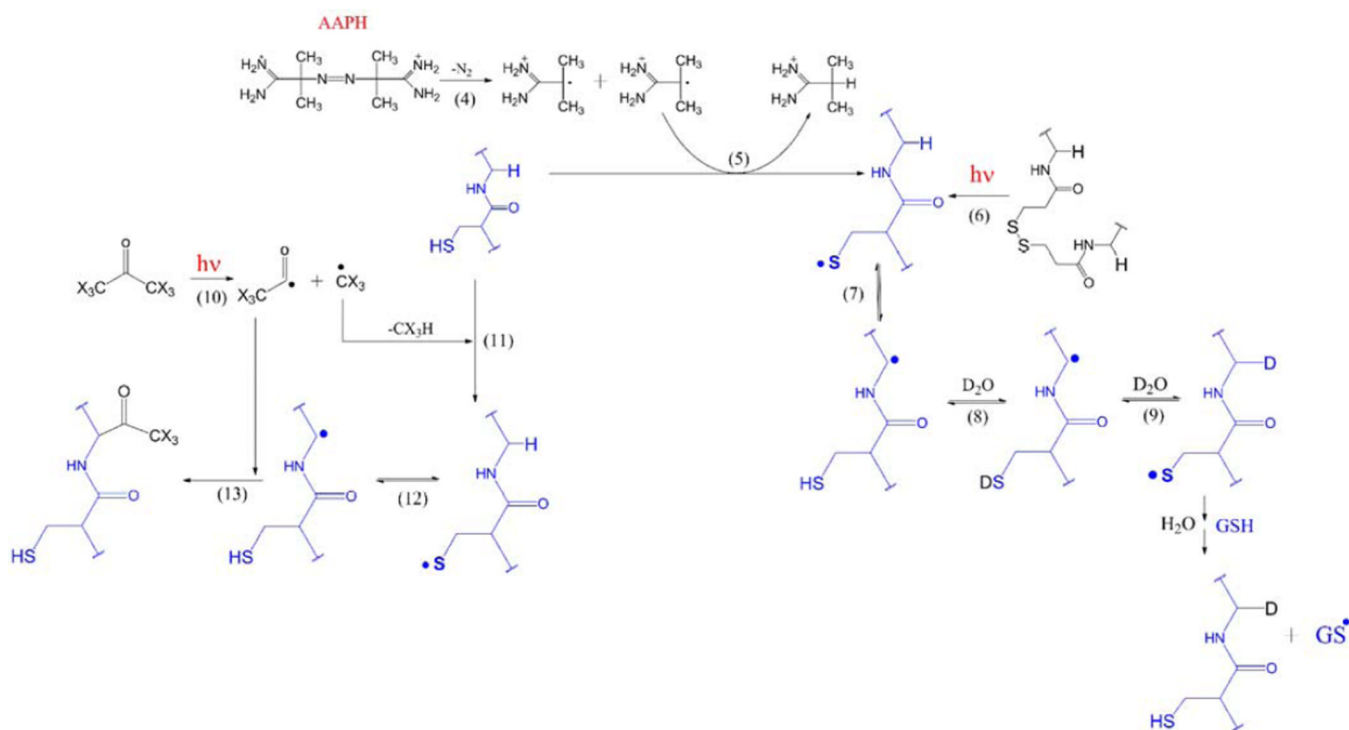
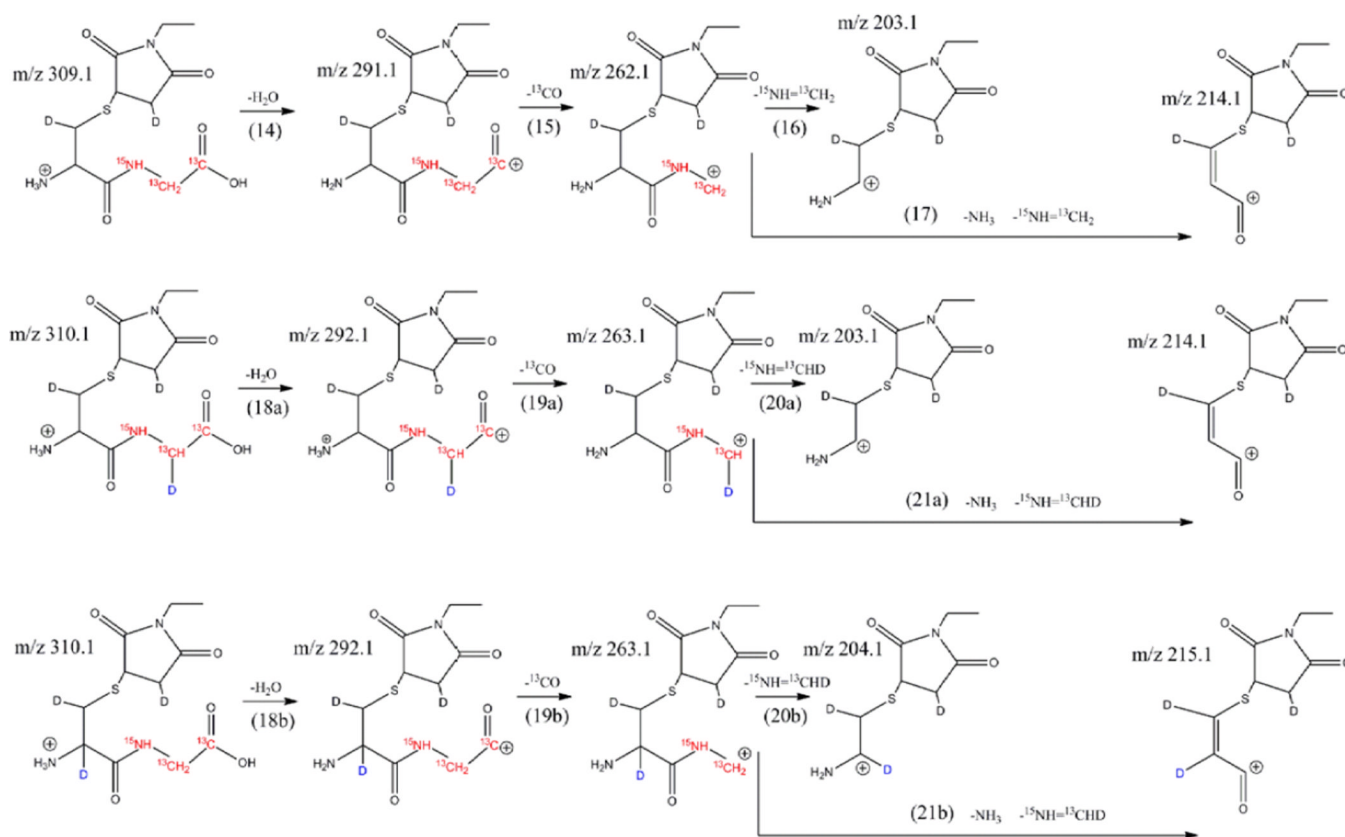


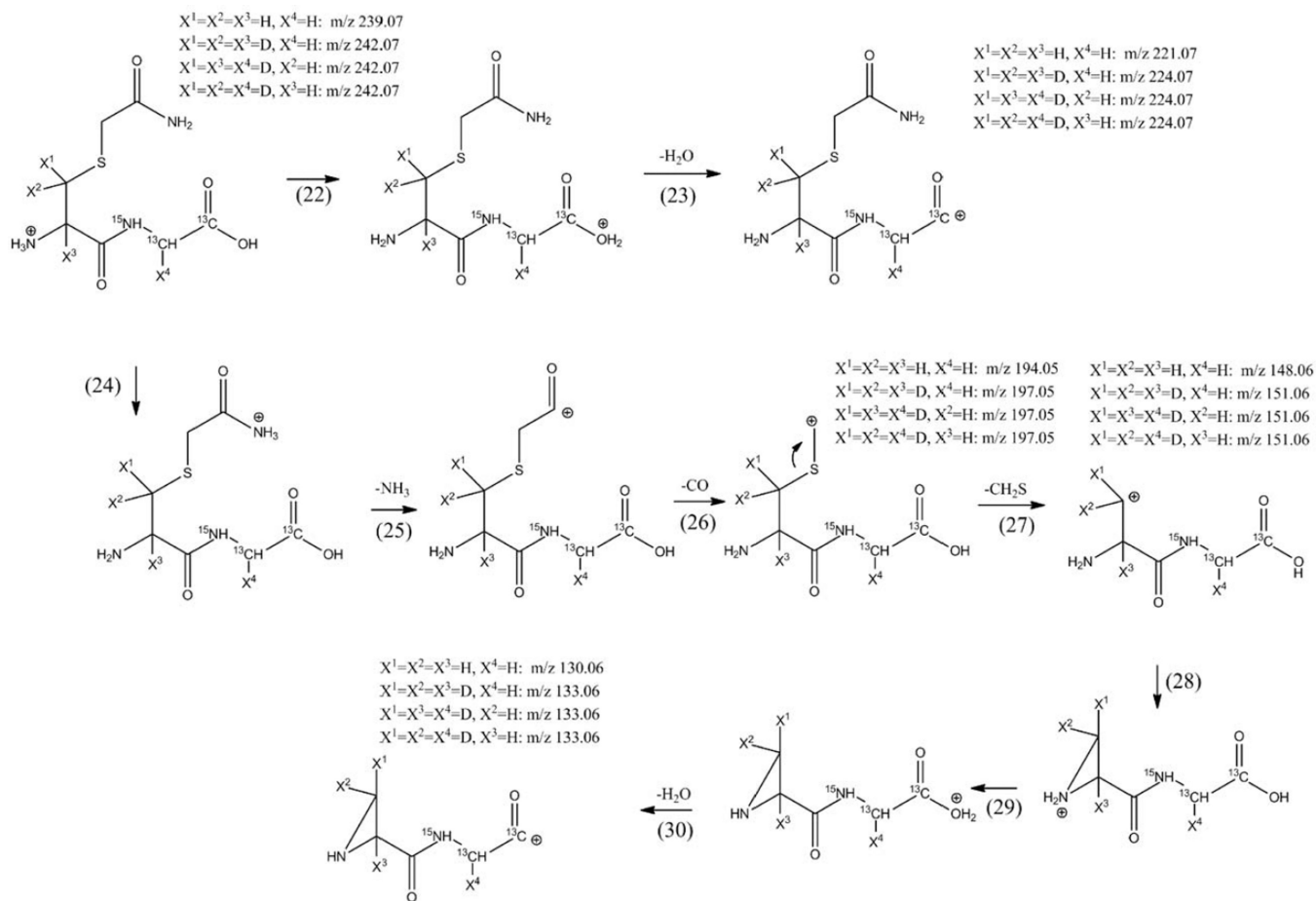
Figure 7. MS³ spectra of the y₂ fragment ions of A) products **4-h-S** and **5-h-Y**, B) products **4-d-S** and **5-d-Y**, and C) products **6-h-S** and **7-h-Y**. The label **Y** refers to the acetylation of GSH or GSH* at the ^αC carbon of Cys, at the ^αC carbon of Gly/Gly* or at the ^βC carbon of Cys.

**Scheme 1.**

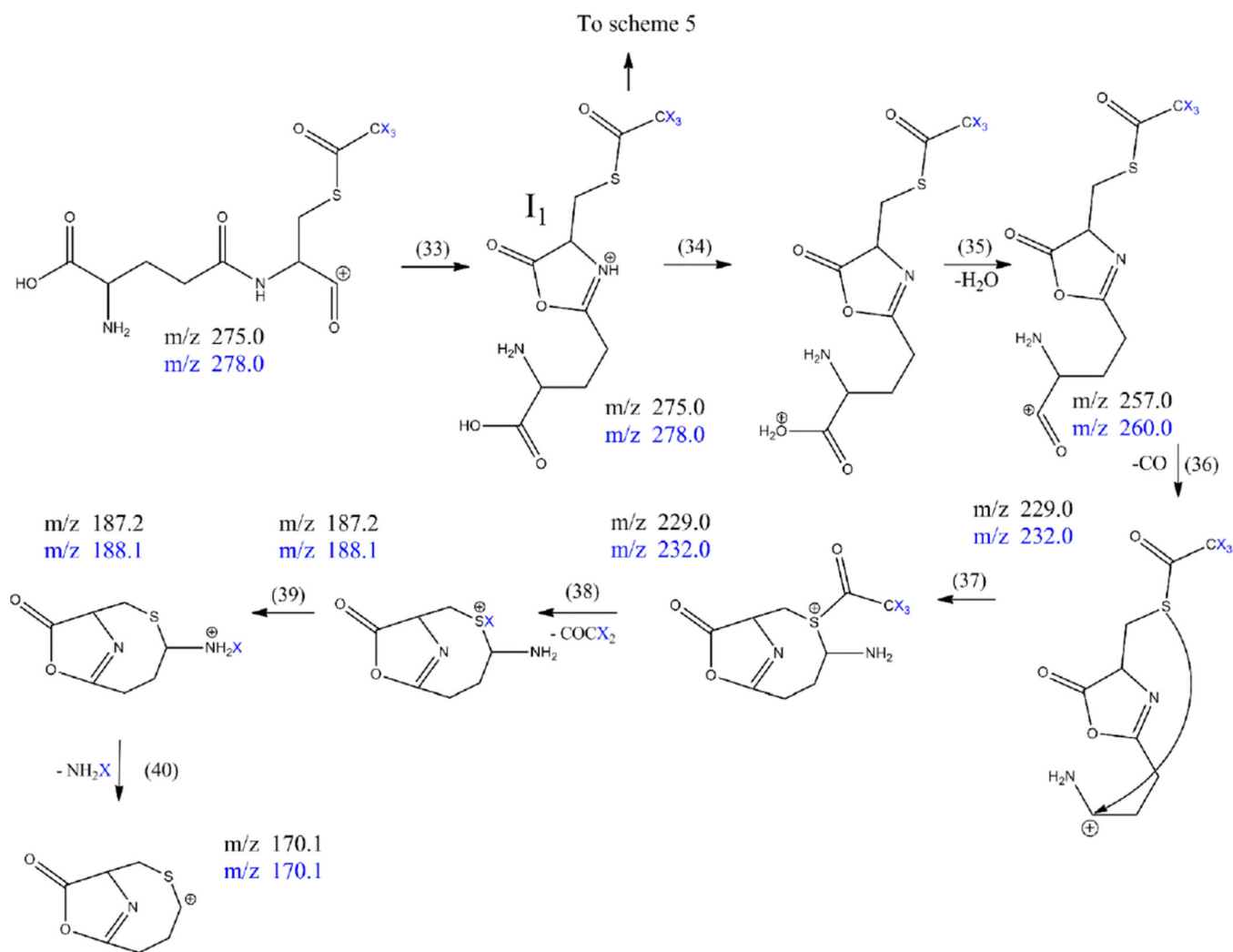
Formation of glutathione thiyl radical using three different protocols, i) the thermal decomposition of AAPH, ii) the photochemistry of disulfide bond, iii) the photochemistry of acetone (X stands for H or D), and subsequent reactions of the thiyl radical.

**Scheme 2.**

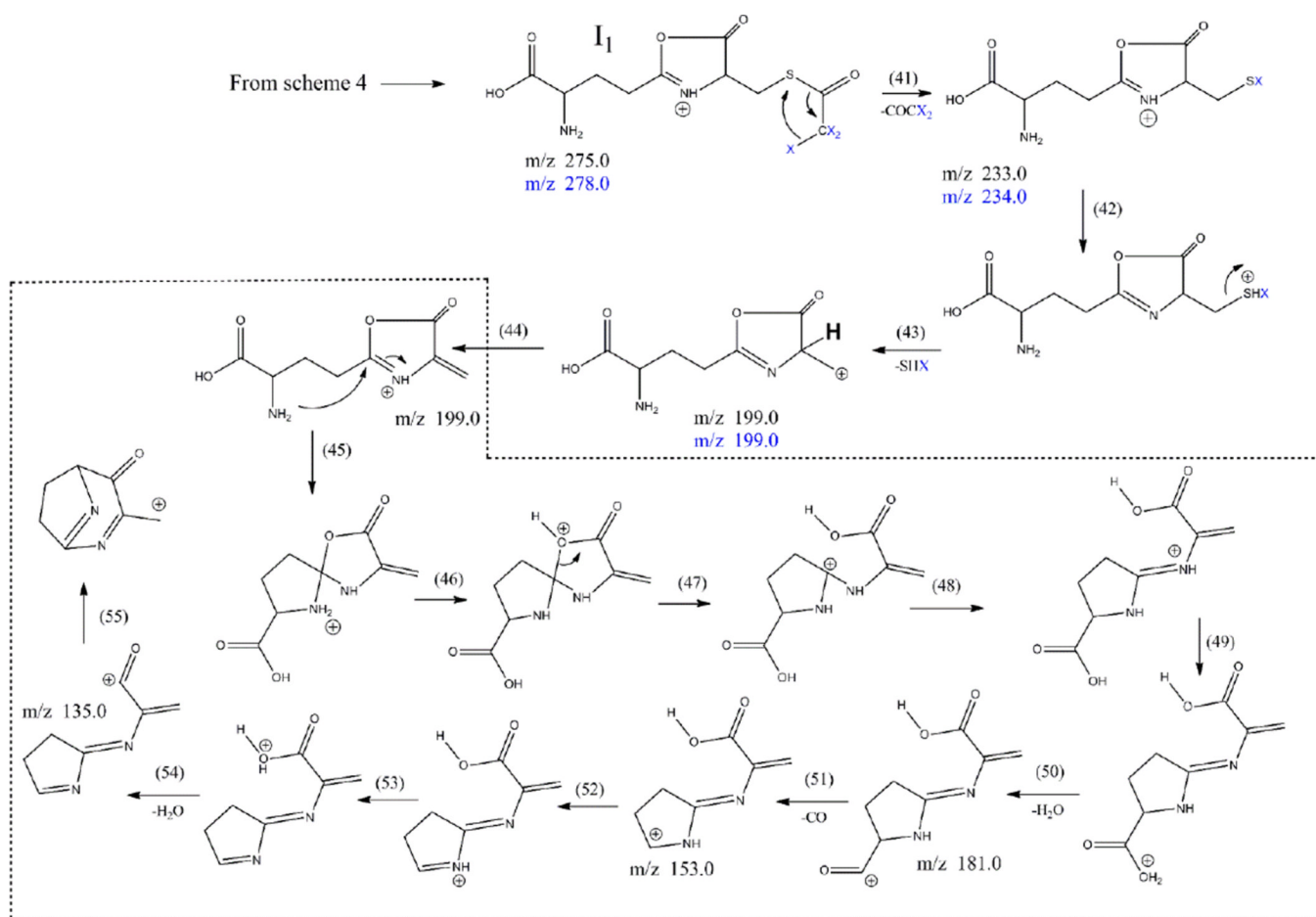
Reaction pathways for the MS³ fragmentation of the y₂ fragment ions of product **2-d-X** after incorporation of two or three deuterons during the reaction of AAPH with GSH/GSH* in D₂O. **X** stands for deuterium incorporation at Cys[^αC], Cys[^βC], or Gly[^αC].

**Scheme 3.**

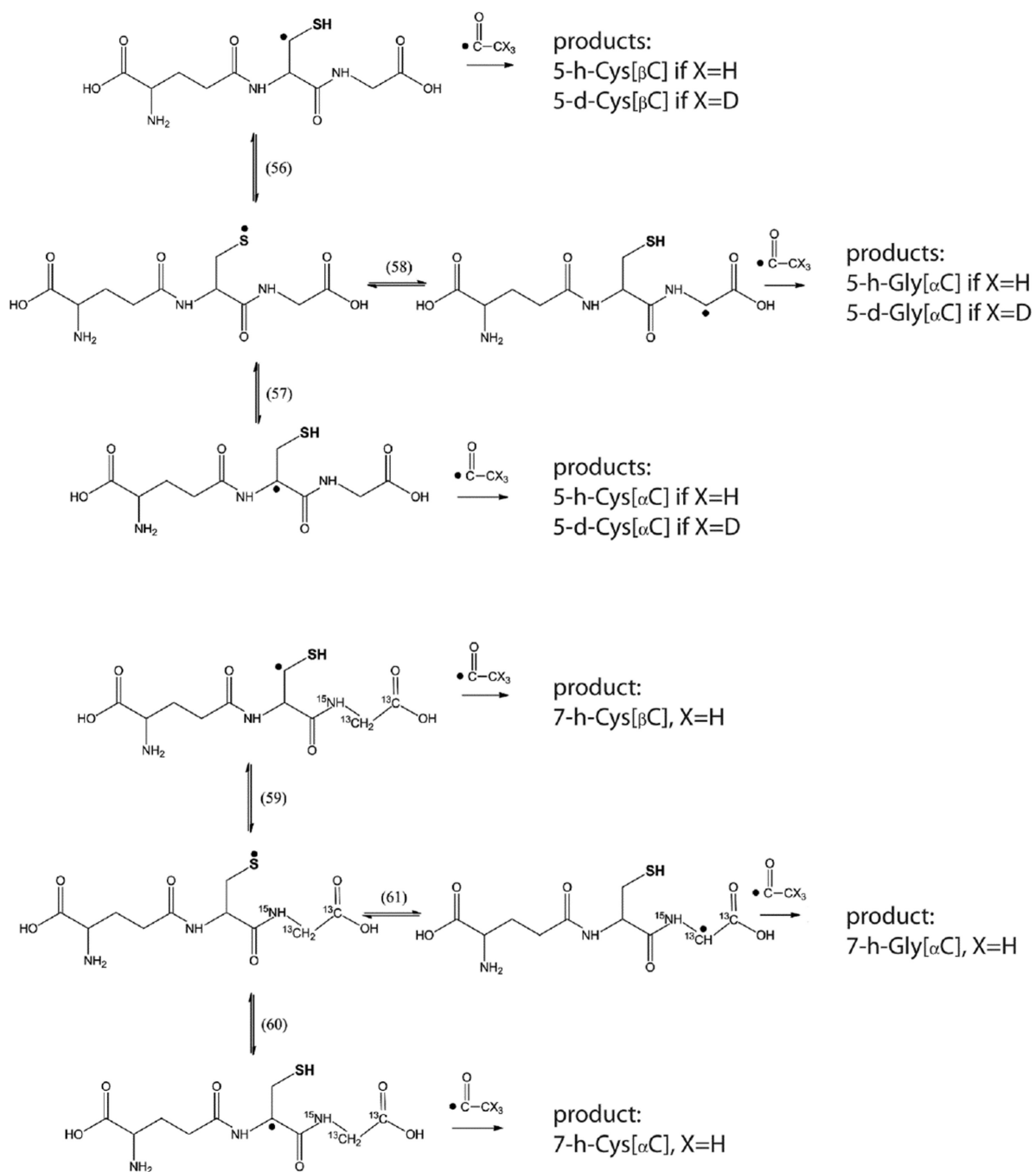
Reaction pathways for the MS³ fragmentation of the y₂ fragment ions of product **3-h** and **3-d-X** after incorporation of three deuterons during the reaction of AAPH with GSH/GSH* in D₂O. **X** stands for deuterium incorporation at Cys[^αC], Cys[^βC], or Gly[^αC].

**Scheme 4.**

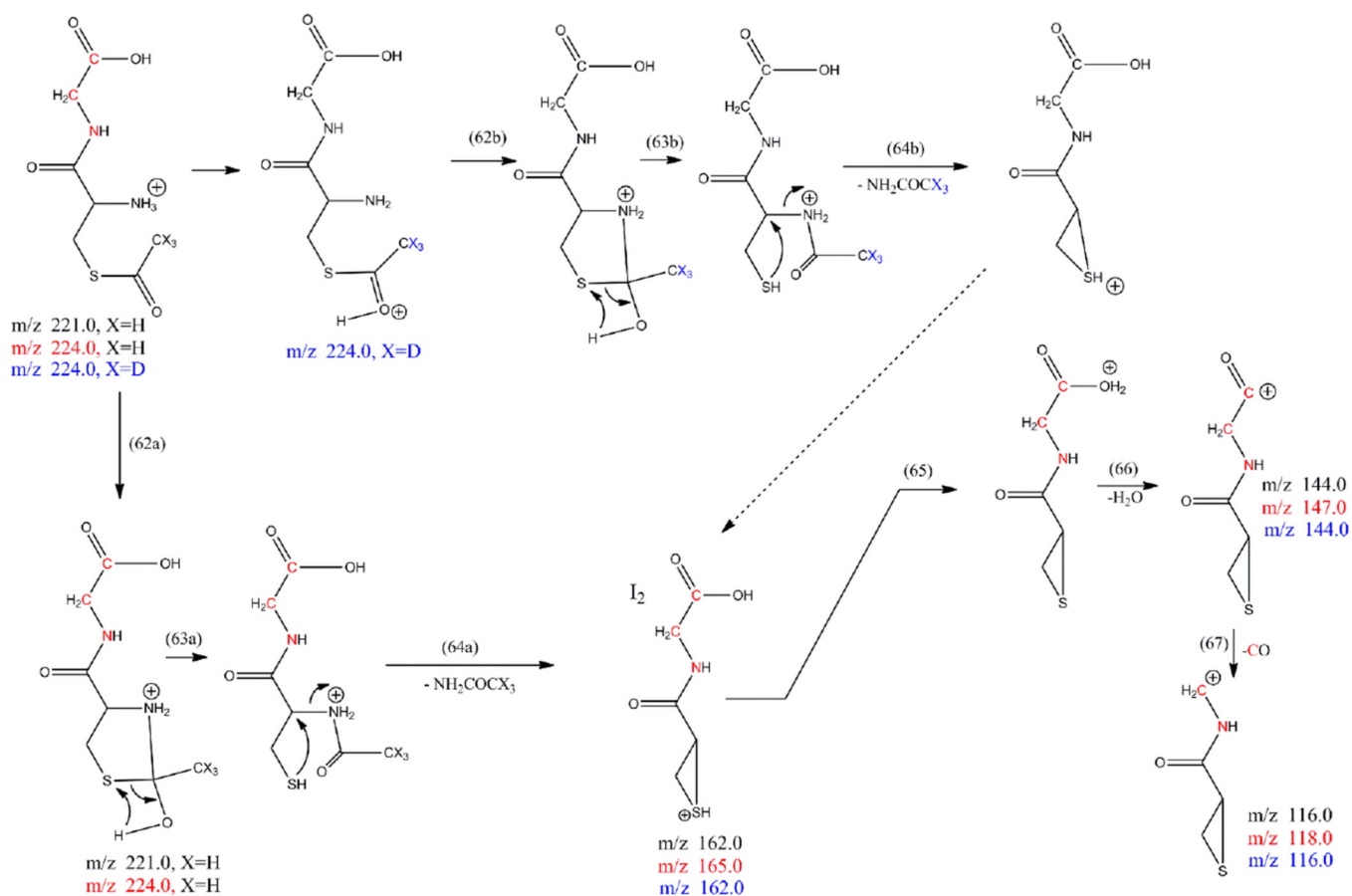
Postulated fragmentation pathway for the MS³ fragmentation of the b₂ fragment ions of products **4-h-S** and **4-d-S**. Color code for m/z : X=H (black), X=D (blue).

**Scheme 5.**

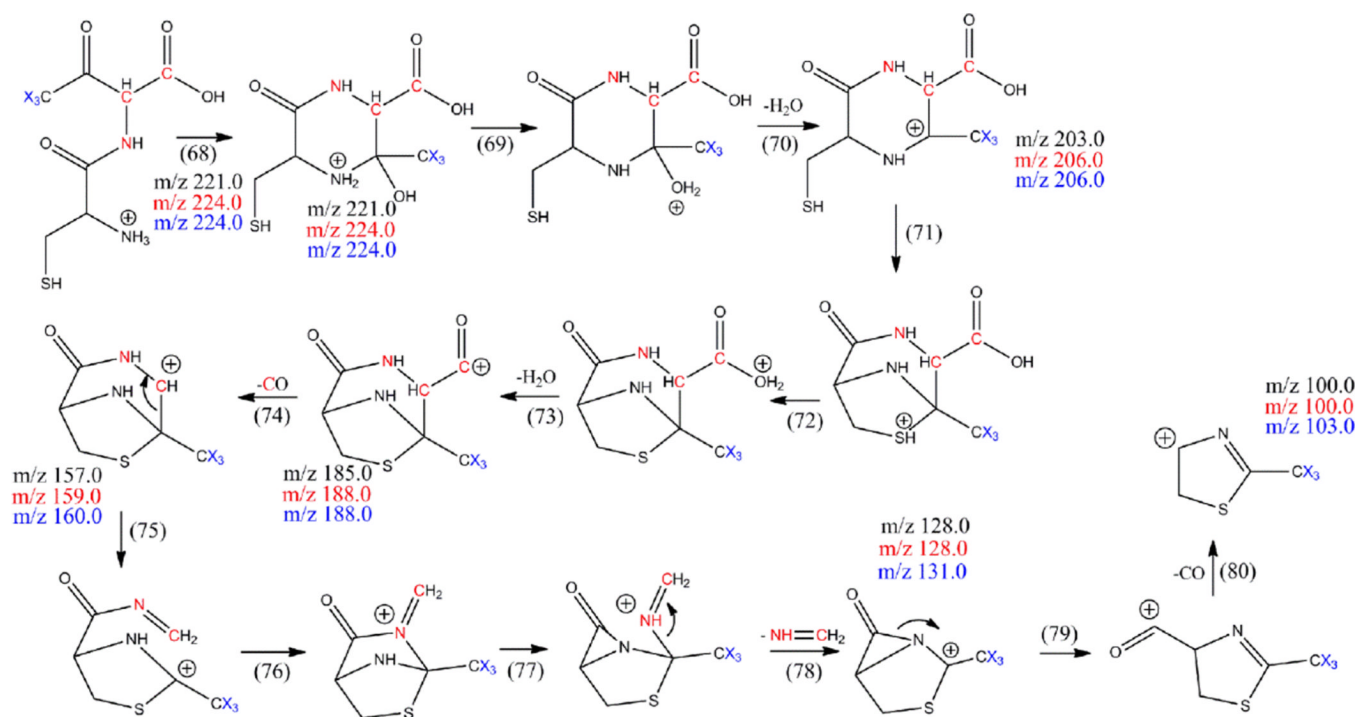
Postulated fragmentation pathways for the MS³ fragmentation of the b₂ fragment ions of products **4-h-S** and **4-d-S** (continued). The dashed frame indicates the MS⁴ fragmentation mechanism of the ion with m/z 199.0. Color code for m/z : X=H (black), X=D (blue).



Scheme 6.
Acetylation of GSH and GSH*.

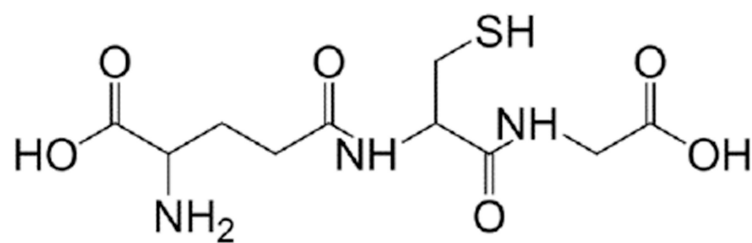
**Scheme 7.**

Postulated fragmentation pathways for the MS³ fragmentation of the y₂ fragment ions of the following products: **4-h-S** (m/z are black colored, and X=H), **4-d-S** (m/z are blue colored, and X=D), **6-h-S** (m/z are red colored, and X=H). The red-colored atoms indicate the position of ¹⁵N and ¹³C when GSH* is used to explain the fragmentation mechanism.

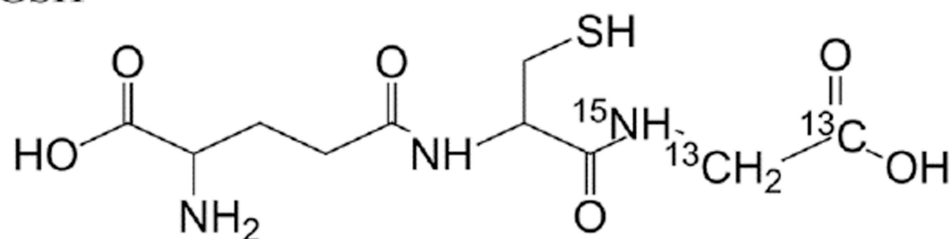
**Scheme 8.**

Postulated fragmentation pathways for the MS³ fragmentation of the y₂ fragment ions of the following products: **5-h-Gly[^αC]** (m/z are black colored), **5-d-Gly[^αC]** (m/z are blue colored), **7-h-Gly[^αC]** (m/z are red colored). The red-colored atoms indicate the position of ¹⁵N and ¹³C when GSH* is used to explain the fragmentation mechanism. The blue-colored atoms indicate either the use of a protonated acetyl radical (X=H) or a deuterated acetyl radical (X=D).

GSH



GSH*



GSSG

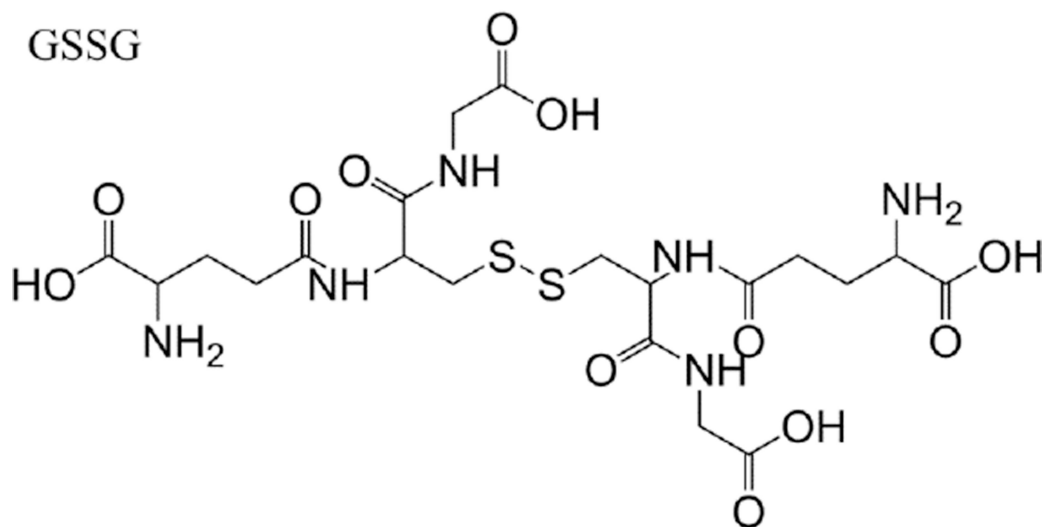


Chart 1.
Structures of glutathione (GSH, GSH*) and GSSG.

Table 1

Overview of the products resulting from the derivatization of GSH with either NEM after reaction of GSH with AAPH. Products **1-d-Cys[α C]**, **1-d-Cys[β C]**, **1-d-Gly[α C]** are products with a second deuterium located on Cys[α C], Cys[β C], Gly[α C], respectively. In the text, the labels Cys[α C], Cys[β C], and Gly[α C] are sometimes represented by the letter X.

Reference	Structure	Reference	Structure
1-h		1-d-Cys[β C]	
1-d-Cys[α C]		1-d-Gly[α C]	

Table 2

Overview of the products resulting from the derivatization of GSH* with either NEM after reaction of GSH* with AAPH. Products **1-d-Cys**[$^{\alpha}\text{C}$], **1-d-Cys**[$^{\beta}\text{C}$], **1-d-Gly**[$^{\alpha}\text{C}$] are products with a second deuterium located on Cys[$^{\alpha}\text{C}$], Cys[$^{\beta}\text{C}$], Gly[$^{\alpha}\text{C}$], respectively. In the text, the labels Cys[$^{\alpha}\text{C}$], Cys[$^{\beta}\text{C}$], and Gly[$^{\alpha}\text{C}$] are sometimes represented by the letter **X**.

Reference	Structure	Reference	Structure
2-h		2-d-Cys[$^{\beta}\text{C}$]	
2-d-Cys[$^{\alpha}\text{C}$]		2-d-Gly[$^{\alpha}\text{C}$]	

Table 3

Overview of the products resulting from the derivatization of GSH with IOA after reaction of GSH with AAPH. Products **1-d-Cys[α C]**, **1-d-Cys[β C]**, **1-d-Gly[α C]** are products with a second deuterium located on Cys[α C], Cys[β C], Gly[α C], respectively. In the text, the labels **Cys[α C]**, **Cys[β C]**, and **Gly[α C]** are sometimes represented by the letter **X**.

Reference	Structure	Reference	Structure
3-h		3-d-Cys[β C]	
3-d-Cys[α C]		3-d-Gly[α C]	

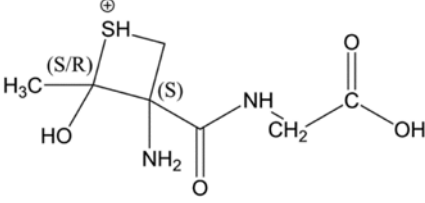
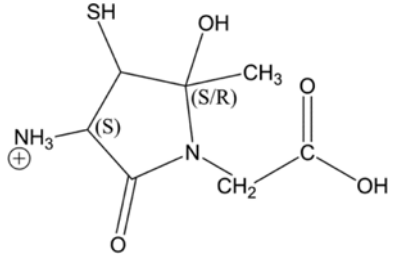
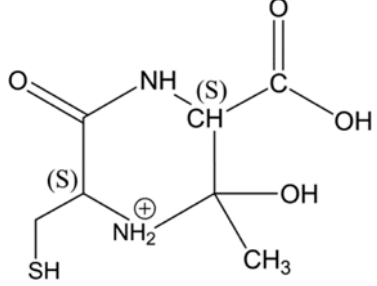
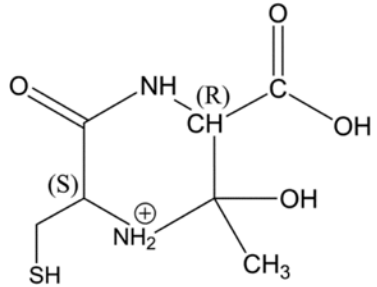
Table 4

Overview of the products resulting from acetone photolysis in the presence of GSH and GSH*. The acetylation on either the α C carbon of Cys, the α C carbon of Gly or the β C carbon of Cys is in the text summarized as **Y** in the name of the product (e.g. **5-h-Y**). When we will refer to one of these products, the **Y** label will be replaced with either the label **Cys[α C]**, **Gly[α C]** (or **Gly[α C¹³]**, in GSH*), or **Cys[β C]**. In this table, a full description of all the possible products **5-h-Y**, **5-d-Y**, and **7-h-Y** is presented.

Reference	Structure	Reference	Structure	Reference	Structure
4-h-S		4-d-S		6-h-S	
5-h-Cys[αC]		5-d-Cys[αC]		7-h-Cys[αC]	
5-h-Cys[βC]		5-d-Cys[βC]		7-h-Cys[βC]	
5-h-Gly[αC]		5-d-Gly[αC]		7-h-Gly[αC¹³]	

Table 5

Structure of the γ_2 ions of products **5-h-Cys**[$^{\alpha}\text{C}$], **5-h-Cys**[$^{\beta}\text{C}$], **5-h-Gly**[$^{\alpha}\text{C}$]. (S) and (R) stand for the absolute configuration chirality of the carbon center.

Product	γ_2 ion after cyclization	Absolute Configuration	G^0_{298} (kcal/mol)
5-h-Cys [$^{\alpha}\text{C}$]		(S,S) (S,R)	No convergence
5-h-Cys [$^{\beta}\text{C}$]		(S,S) (S,R)	29.49 15.69
5-h-Gly [$^{\alpha}\text{C}$] Gly[$^{\alpha}\text{C}$] has a S configuration after addition of the acetyl radical		(S,S,S) (S,S,R)	1.88 1.25
5-h-Gly [$^{\alpha}\text{C}$] Gly[$^{\alpha}\text{C}$] has a R configuration after addition of the acetyl radical		(S,R,S) (S,R,R)	3.14 0.00